DOI: 10.1002/chem.200501540

Synthesis, Structure, and Reactivity of Palladacycles That Contain a Chiral Rhenium Fragment in the Backbone: New Cyclometalation and Catalyst Design Strategies

Florian K. Friedlein, Klemenz Kromm, Frank Hampel, and J. A. Gladysz*[a]

Abstract: The bromocyclopentadienyl complex $[(\eta^5\text{-}C_5H_4Br)Re(CO)_3]$ is converted to racemic $[(\eta^5\text{-}C_5H_4Br)Re(NO)(PPh_3)(CH_2PPh_2)]$ (**1b**) similarly to a published sequence for cyclopentadienyl analogues. Treatment of enantiopure (*S*)-$[(\eta^5\text{-}C_5H_5)Re(NO)(PPh_3)(CH_3)]$ with *n*BuLi and I_2 gives (*S*)-$[(\eta^5\text{-}C_5H_4I)Re(NO)(PPh_3)(CH_3)]$ ((*S*)-**6c**; 84%), which is converted ($Ph_3C^+PF_6^-$, PPh_2H, *t*BuOK) to (*S*)-$[(\eta^5\text{-}C_5H_4I)Re(NO)(PPh_3)(CH_2PPh_2)]$ ((*S*)-**1c**). Reactions of **1b** and (*S*)-**1c** with $Pd[P(t\text{Bu})_3]_2$ yield $[\{(\eta^5\text{-}C_5H_4)Re(NO)(PPh_3)(\mu\text{-}CH_2PPh_2)Pd(\mu\text{-}X)\}_2]$ (**10**; X = **b**, Br, *rac*/*meso*, 88%; **c**, I, *S*,*S*, 22%). Addition of PPh_3 to **10b** gives $[(\eta^5\text{-}C_5H_4)Re(NO)(PPh_3)(\mu\text{-}CH_2PPh_2)Pd(PPh_3)(Br)]$ (**11b**; 92%). Reaction of (*S*)-$[(\eta^5\text{-}C_5H_5)Re(NO)(PPh_3)(CH_2PPh_2)]$ ((*S*)-**2**) and $Pd(OAc)_2$ (1.5 equiv; toluene, RT) affords the novel $Pd_3(OAc)_4$-based palladacycle (*S*,*S*)-$[(\eta^5\text{-}C_5H_4)Re(NO)(PPh_3)(\mu\text{-}CH_2PPh_2)Pd(\mu\text{-}OAc)_2Pd(\mu\text{-}OAc)_2Pd(\mu\text{-}PPh_2CH_2)(Ph_3P)(ON)Re(\eta^5\text{-}C_5H_4)]$ ((*S*,*S*)-**13**; 71–90%). Addition of LiCl and LiBr yields (*S*,*S*)-**10a**,**b** (73%), and $Na(acac\text{-}F_6)$ gives (*S*)-$[(\eta^5\text{-}C_5H_4)Re(NO)(PPh_3)(\mu\text{-}CH_2PPh_2)Pd(acac\text{-}F_6)]$ ((*S*)-**16**, 72%). Reaction of (*S*,*S*)-**10b** and pyridine affords (*S*)-$[(\eta^5\text{-}C_5H_4)Re(NO)(PPh_3)(\mu\text{-}CH_2PPh_2)Pd(NC_5H_5)(Br)]$ ((*S*)-**17b**, 72%); other Lewis bases yield similar adducts. Reaction of (*S*)-**2** and $Pd(OAc)_2$ (0.5 equiv; benzene, 80°C) gives the spiropalladacycle *trans*-(*S*,*S*)-$[\{(\eta^5\text{-}C_5H_4)Re(NO)(PPh_3)(\mu\text{-}CH_2PPh_2)\}_2Pd]$ (39%). The crystal structures of (*S*)-**6c**, **11b**, (*S*,*S*)- and (*R*,*R*)-**13**·$2C_7H_8$, (*S*,*S*)-**10b**, and (*S*)-**17b** aid the preceding assignments. Both **10b** (racemic or *S*,*S*) and (*S*)-**16** are excellent catalyst precursors for Suzuki and Heck couplings.

Keywords: cyclometalation · Heck reaction · palladacycle · palladium · rhenium · Suzuki coupling

Introduction

Although palladacycles that feature a neutral heteroatomic donor atom and a palladium–carbon σ bond have been known and studied for over 40 years,[1] there has been a marked surge of interest in the last decade.[2] Such palladacycles are most commonly prepared by donor-atom-templated insertions into carbon–hydrogen or carbon–halogen bonds. However, many other synthetic routes have been developed.

Much of this recent activity has been prompted by the increasing use of palladacycles as catalyst precursors, particularly for carbon–carbon bond-forming reactions.[2] Certain complexes effect extraordinarily high turnover numbers ($> 10^6$), typically in coupling reactions involving aryl halides.[2,3] Chiral palladacycles have also been synthesized in enantiomerically pure form and employed in enantioselective transformations.[4,5]

We have had a long-standing interest in catalysts that contain "spectator" metal fragments: in other words, ligand-based metals that do not participate directly in the catalytic cycle but whose steric and/or electronic properties may play important roles.[6–10] A variety of palladacycles that incorporate ferrocenyl or ruthenocenyl moieties have been reported.[4,11] However, only a handful with other types of metallic units have been synthesized.[5,12,13] Representative examples are mentioned in the Discussion section. Some of these bimetallic palladacycles have been applied in catalysis,[4,5] whereas others have been synthesized with different objectives in mind.

[a] F. K. Friedlein, Dr. K. Kromm, Dr. F. Hampel, Prof. Dr. J. A. Gladysz
Institut für Organische Chemie
Friedrich-Alexander-Universität Erlangen–Nürnberg
Henkestrasse 42, 91054 Erlangen (Germany)
Fax: (+49) 9131-852-6865
E-mail: gladysz@organik.uni-erlangen.de

Supporting information for this article, including data on starting chemicals, additional palladacycles characterized in situ, and Mizoroki–Heck reactions, is available on the WWW under http://www.chemeurj.org/ or from the author.

We speculated that new types of palladacycles might be generally available from half-sandwich complexes **I** and **II** (Scheme 1). These easily accessed building blocks feature ligands containing donor atoms $-CH_2-D:$ ($-D:$ = halide, alkoxide, thioalkoxide, amide, phosphide) capable of binding a palladium precursor. For **I**, coordination of palladium(0) would be followed by an oxidative addition involving the halocyclopentadienyl ligand, giving the target species **III**. For **II**, coordination of palladium(II) would be followed by carbon–hydrogen bond activation and HX elimination.[2,14] Alternatively, alkylcyclopentadienyl complexes with M–D: linkages might be employed similarly, as illustrated for the pentamethylcyclopentadienyl adduct **IV**.

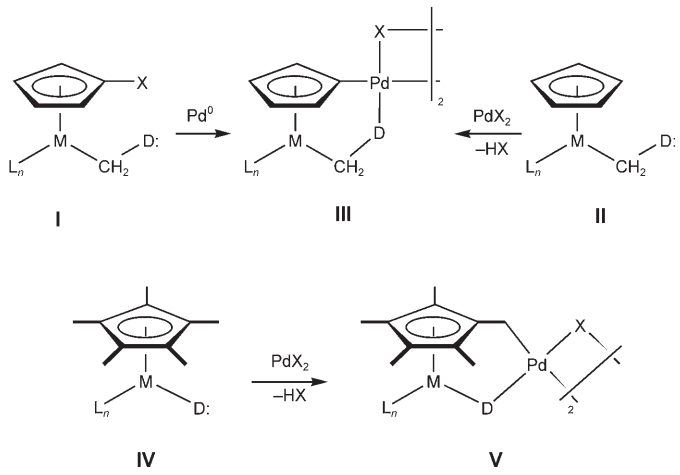

Scheme 1. Synthetic planning: palladacycles that contain a transition metal in the backbone.

Importantly, such cyclopentadienyl complexes are easily rendered chiral. Given the broad utility of palladacycles in catalysis, there is strong interest in the development of new chirality motifs.[4,5,11,12] Herein, we report a) the successful application of the strategies in Scheme 1 to produce racemic and enantiomerically pure "chiral-at-metal" rhenium complexes $[(\eta^5\text{-}C_5H_4X)Re(NO)(PPh_3)(CH_2PPh_2)]$ (X = halide, **1**; X = H, **2**), which feature phosphorus donor atoms; b) the detailed structural characterization of the resulting palladacycles, including an unusual species with a tripalladium core; and c) the use of these palladacycles as catalyst precursors for Suzuki–Miyaura and Mizoroki–Heck reactions. Some of this work has been communicated.[10]

Results

Synthesis of halocyclopentadienyl complexes: At the outset of this work, we expected the more reliable route to palladacycles **III** to be from halocyclopentadienyl complexes **I**. We therefore sought to adapt previous syntheses of the racemic and enantiomerically pure parent compound $[(\eta^5\text{-}C_5H_5)Re(NO)(PPh_3)(CH_2PPh_2)]$ (**2**)[7a] from $[(\eta^5\text{-}C_5H_5)Re(CO)_3]$ to brominated and iodinated analogues $[(\eta^5\text{-}C_5H_4X)Re(NO)(PPh_3)(CH_2PPh_2)]$ (**1b**,**c**).[15] The bromocyclopentadienyl complex $[(\eta^5\text{-}C_5H_4Br)Re(CO)_3]$ (**3b**) is readily available.[16] Also, rhenium cyclopentadienyl complexes are often easily converted to lithiocyclopentadienyl complexes,[7a,b,9a,17] which can be functionalized with electrophiles. Accordingly, two approaches to the requisite halocyclopentadienyl species were investigated.

Reaction of the bromocyclopentadienyl complex **3b** and $NO^+BF_4^-$ (Scheme 2) gave the nitrosyl complex $\mathbf{4b}^+BF_4^-$ (86%).[15] Treatment of $\mathbf{4b}^+BF_4^-$ with PPh_3 in refluxing CH_2Cl_2 yielded the racemic chiral phosphine complex $\mathbf{5b}^+BF_4^-$ (68%). This substitution proceeded under much milder conditions than with the cyclopentadienyl analogue.[18] Subsequent reduction with $NaBH_4$ gave the methyl complex **6b** (82%), which was stable for over a year in air, in contrast to the cyclopentadienyl analogue, which decomposes slowly over the course of several weeks.

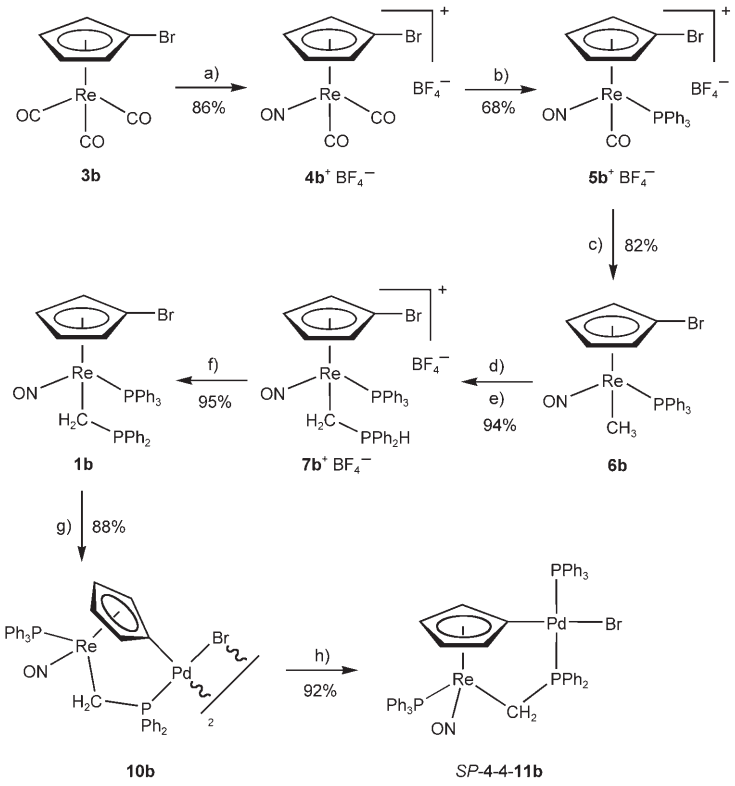

Scheme 2. Syntheses of racemic palladacycles via bromocyclopentadienyl rhenium complexes: a) $NO^+BF_4^-$, CH_2Cl_2, −15°C; b) PPh_3, CH_2Cl_2, reflux; c) $NaBH_4$, THF, RT; d) 1.1 equiv $Ph_3C^+BF_4^-$, CH_2Cl_2, −60°C; e) 1.1 equiv PPh_2H, −60°C to RT; f) 1.2 equiv *t*BuOK, THF, RT; g) 1.0 equiv $Pd[P(tBu)_3]_2$, toluene, 80°C; h) PPh_3, CH_2Cl_2, RT.

Complex **6b** was treated sequentially with $Ph_3C^+BF_4^-$ and PPh_2H. Workup gave the phosphonium salt $\mathbf{7b}^+BF_4^-$ (94%; Scheme 2). Deprotonation with *t*BuOK afforded the target complex **1b** (95%) as orange prisms. This compound was also less air-sensitive than its cyclopentadienyl analogue

2, suggesting a general effect of the electron-withdrawing bromide substituent.

The new complexes in Scheme 2, and all the others that were isolated as part of this study, were characterized by IR and NMR spectrometry, mass spectrometry, and microanalysis, as summarized in the Experimental Section. Most features were routine, and have been analyzed in greater detail elsewhere.[19] In the chiral complexes (**1b**, **5b**$^+$ BF_4^-, **6b**, **7b**$^+$ BF_4^-) the two cyclopentadienyl CH groups α and β to the bromide substituents are diastereotopic. Accordingly, ^{1}H NMR spectra exhibited four broad singlets or multiplets. Similarly, ^{13}C NMR spectra gave five cyclopentadienyl carbon signals.

A second synthetic approach to halocyclopentadienyl complexes is summarized in Scheme 3. The enantiopure

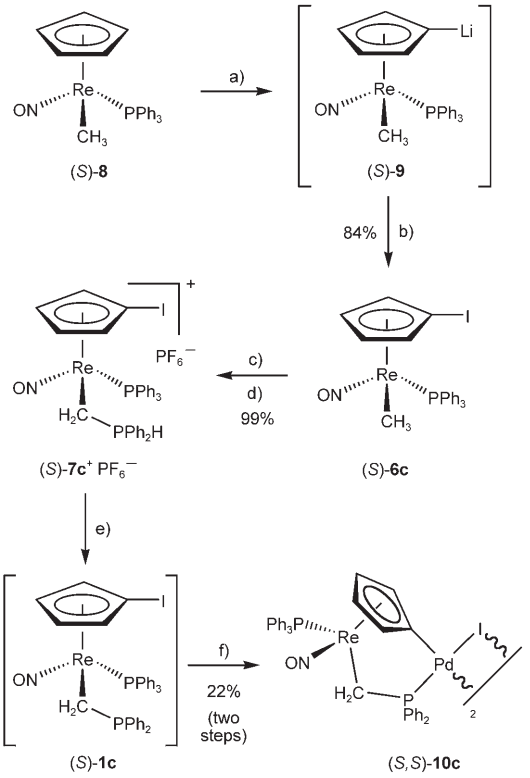

Scheme 3. Syntheses of enantiopure palladacycles via iodocyclopentadienyl rhenium complexes: a) 1.0 equiv *n*BuLi, THF, −78 °C to RT; b) 1.0 equiv I_2, THF, −78 °C; c) 1.1 equiv Ph_3C^+ PF_6^-, CH_2Cl_2, −78 °C; d) 1.8 equiv PPh_2H, −78 °C to RT; e) 1.5 equiv *t*BuOK, toluene, RT; f) 1.0 equiv $Pd[P(tBu)_3]_2$, toluene, RT.

methyl complex **8** and *n*BuLi react to give the enantiopure lithiocyclopentadienyl complex **9**.[17a] Thus, (*S*)-**8** was sequentially treated with *n*BuLi (−78 °C, then RT) and I_2 (−78 °C). Workup gave the iodocyclopentadienyl complex (*S*)-**6c** (84 %).[15] This was treated with Ph_3C^+ PF_6^- and PPh_2H similarly to **6b**, giving the phosphonium salt (*S*)-**7c**$^+$ PF_6^- (99 %). Deprotonation to the target complex (*S*)-**1c** was effected in conjunction with the cyclopalladations described below.

Rd cubes of (*S*)-**6c** were obtained from benzene/hexanes, and X-ray data were collected (see Table 1 and the Experimental Section). Refinement gave the molecular structure depicted in Figure 1, confirming the rhenium configuration assigned above, which corresponds to retention from (*S*)-**8**. In accord with abundant precedent, all the other transformations in this paper are presumed to occur with retention at rhenium.[7,17b] Key bond lengths and angles in (*S*)-**6c** are summarized in Figure 1. For most of the nonracemic complexes in this paper, both enantiomers were synthesized.[20]

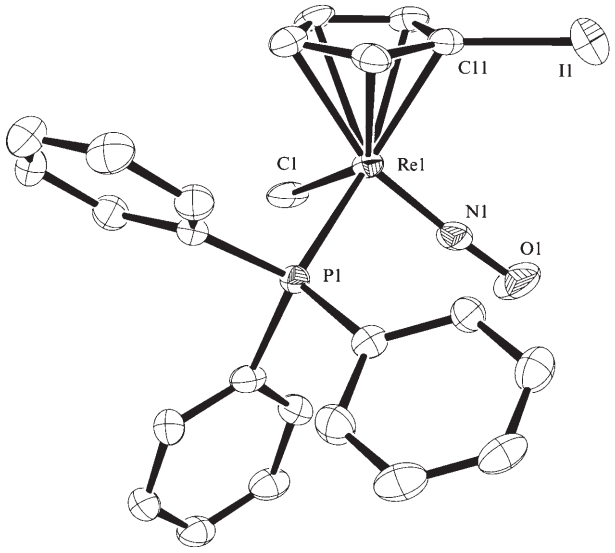

Figure 1. Molecular structure of (*S*)-**6c**. Key distances [Å] and angles [°]: Re1−N1 1.755(4), Re1−P1 2.3348(11), Re1−C1 2.237(5), Re1−C11 2.252(5), C11−I1 2.084(4), N1−O1 1.209(5); P1-Re1-N1 92.68(13), N1-Re1-C1 94.6(2), C1-Re1-P1 92.42(17), Re1-C11-I1 123.9(2).

Palladacycles from halocyclopentadienyl complexes: Experiments were first conducted with the racemic bromocyclopentadienyl complex **1b** and the commercially available palladium bis(phosphine) complex $[Pd\{P(tBu)_3\}_2]$. The latter is known to undergo particularly facile phosphine displacement.[21] Reaction in toluene at 80 °C (Scheme 2, bottom) led to the target palladacycle **10b** (88 %). This material was thermally very stable (decomp 294 °C), but poorly soluble in organic solvents. The dimeric structure was evidenced by a molecular ion in the mass spectrum.

Complex **10b** features two rhenium stereocenters. Hence, configurational diastereomers (*rac*/*meso*) are possible, as well as *syn*/*anti* isomers about the Pd_2Br_2 core. The ^{31}P NMR spectrum showed four pairs of PPh_3 and CH_2PPh_2 signals (all doublets) with area ratios of approximately 69:69:31:31. In view of the data below for enantiomerically pure (*S*,*S*)-**10b**, the two major signals must be *rac* and *meso* diastereomers of one *syn*/*anti* isomer, and the two minor signals analogous diastereomers of the other. Thus, there is negligible chiral recognition across the nearly planar Pd_2Br_2 core (see below). The ^{1}H NMR spectrum of **10b** and most palladacycles below showed one cyclopentadienyl proton with a chemical shift distinctly upfield of the others (δ = 2.80–2.86 versus 4.72–5.47 ppm).[22]

Table 1. Summary of crystallographic data.[a]

Complex	(*S*)-**6c**	*SP*-4-4 **11b**·2 CH_2Cl_2	(*S*,*S*)-**13**·2 C_7H_8[b]	*anti*-(*S*,*S*)-**10b**·CH_2Cl_2·2 $CHCl_3$	*SP*-4-2 (*S*,*S*)-**17b**·$CHCl_3$
molecular formula	$C_{24}H_{22}INOPRe$	$C_{56}H_{50}BrCl_4NOP_3PdRe$	$C_{94}H_{90}N_2O_{10}P_4Pd_3Re_2$	$C_{75}H_{66}Br_2Cl_8N_2O_2P_4Pd_2Re_2$	$C_{42}H_{37}Br_2Cl_3N_2OP_2PdRe$
molecular weight	684.5	1360.2	2223.16	2179.80	1126.54
diffractometer	Kappa CCD	Nonius MACH3	Kappa CCD	Kappa CCD	Kappa CCD
crystal system	orthorhombic	triclinic	orthorhombic	orthorhombic	orthorhombic
space group	$P2_12_12_1$	$P\bar{1}$	$P2_12_12_1$	$P2_12_12_1$	$P2_12_12_1$
a [Å]	9.0140(2)	13.512(3)	14.6308(2)	14.0864(3)	9.6911(2)
b [Å]	14.2060(3)	14.098(3)	23.2935(2)	29.3197(5)	15.6896(3)
c [Å]	17.7350(2)	16.710(3)	25.5324(4)	9.7284(2)	28.0415(4)
α [°]	90	69.57(3)	90	90	90
β [°]	90	77.05(3)	90	90	90
γ [°]	90	74.73(3)	90	90	90
V [Å^3]	2271.02(7)	2846.6(10)	8701.5(2)	4017.92(14)	4263.70(13)
Z	4	2	4	2	4
ρ_{calcd} [Mg m^{-3}]	2.002	1.587	1.697	1.802	1.755
μ [mm^{-1}]	6.796	3.452	3.513	4.828	4.755
F(000)	1296	1340	4384	2108	2192
crystal size [mm]	0.30×0.25×0.20	0.20×0.20×0.20	0.10×0.05×0.05	0.30×0.20×0.20	0.30×0.20×0.10
θ range [°]	1.84 to 27.50	2.62 to 26.33	2.29 to 27.51	1.39 to 27.49	1.45 to 27.46
index ranges (*h*;*k*;*l*)	−11,11;−18,18;−22,23	−16,16;−17,0;−20,19	−18,18;−30,30;−33,33	−18,18; −37,38; −12,12	−12,12; −20,20; −36,36
reflections collected	5175	12037	19866/19799	9169	9599
independent reflections	5175	11546 [*R*(int) = 0.0810]	19866	9169	9599
reflections [$I>2\sigma(I)$]	4919	8262	15145	7719	8324
completeness to θ = 27.47°	99.9% (θ = 27.50°)	99.7% (θ = 26.33°)	99.6%	99.9%	99.0%
max. and min. transmission	0.3435 and 0.2350	0.5452 and 0.5452	0.8439 and 0.7202	0.4452 and 0.3253	0.6622 and 0.3459
data/restraints/parameters	5175/0/262	11546/0/613	19866/19/1036	9169/0/451	9599/0/478
goodness-of-fit on F^2	1.058	1.059	0.981	1036	1087
final *R* indices [$I>2\sigma(I)$]	R_1 = 0.0240 wR_2 = 0.0550	R_1 = 0.0468 wR_2 = 0.1122	R_1 = 0.0418 wR_2 = 0.0820	R_1 = 0.0475 wR_2 = 0.1222	R_1 = 0.0384 wR_2 = 0.0846
R indices (all data)	R_1 = 0.0265 wR_2 = 0.0557	R_1 = 0.0875 wR_2 = 0.1338	R_1 = 0.0717 wR_2 = 0.0921	R_1 = 0.0610 wR_2 = 0.1331	R_1 = 0.0503 wR_2 = 0.0929
absolute structure (Flack) parameter	0.013(6)	–	−0.010(4)	−0.030(9)	−0.009(6)
largest diff. peak/hole [e Å^{-3}]	0.700/−1.045	1.691/−1.363	0.963/−0.889	2.656/−1.056	0.981/−1.126

[a] Data common to all structures: temp. of collection [K] = 173(2); wavelength [Å] = 0.71073; refinement method: full-matrix least-squares on F^2. [b] Key data for the enantiomer (*R*,*R*)-**13**·2 C_7H_8 (Ref. [10]): *a*/*b*/*c* [Å] = 14.63350(10)/23.3173(2)/25.5322(2); *V* [Å^3] = 8711.94(12); ρ_{calcd} [Mg m^{-3}] = 1.695; goodness-of-fit = 1.066; final *R* indices [$I>2\sigma(I)$], R_1 = 0.0288 and wR_2 = 0.0693; *R* indices (all data), R_1 = 0.0398 and wR_2 = 0.0865.

A more soluble and monomeric palladacycle was sought. The reaction of **10b** and PPh_3 (Scheme 2) afforded **11b** (92%). Although two geometric isomers are possible at palladium, only one was detected in solution. As observed for other palladacycles described below, the ^{13}C NMR signal of the palladium-bound cyclopentadienyl carbon atom (δ = 143.1 ppm) was far downfield from the others (δ = 92.6–85.6 ppm). The crystal structure of a solvate was determined (Table 1 and the Experimental Section). Key bond lengths and angles are listed in Table 2. The bromide ligand is *trans* to the cyclopentadienyl ligand (Figure 2), which according to modern nomenclature conventions can be designated as an *SP*-4-4 isomer.[23]

An analogous cyclopalladation was attempted with the enantiopure iodocyclopentadienyl complex (*S*)-**1c**. This compound was first generated in situ from (*S*)-**7c**$^+$ PF_6^- and *t*BuOK (Scheme 3). Crystal structures of the corresponding cyclopentadienyl complexes have rigorously established retention of configuration at rhenium.[7a] Subsequent addition of [Pd{P(*t*Bu)$_3$}$_2$] gave the bridging iodide complex (*S*,*S*)-**10c** in 22% overall yield (unoptimized) as a 21:79 mixture of *syn*/*anti* isomers. The spectroscopic properties were very similar to those of **10b**.

Palladacycles from cyclopentadienyl complexes: The phosphonium salt (*S*)-**12**$^+$ PF_6^-, *t*BuOK (1.2 equiv), and Pd(OAc)$_2$ (1.5 equiv) were combined in toluene (Scheme 4). The first two reactants are known to generate (*S*)-**2**,[7a,9a] and the last has been used to synthesize many dimeric $Pd_2(OAc)_2$-based palladacycles from organic heteroatom donors. Workup gave a palladacyclic product in high yield, as indicated by characteristic NMR data as described above. The ^1H NMR, ^{13}C NMR, and IR spectra clearly showed the presence of acetate residues. The same complex was ob-

Table 2. Key interatomic distances [Å] and angles [°] for rhenium-containing palladacycles.

	SP-4-4 **11b**	(*S*,*S*)-**13**/(*R*,*R*)-**13**	*anti*-(*S*,*S*)-**10b**	*SP*-4-2 (*S*)-**17b**
Pd1−C11	2.010(7)	1.985(7)/1.983(5)	1.994(8)	1.989(6)
Pd1−P1	2.287(2)	2.2007(19)/2.1988(14)	2.224(2)	2.2338(18)
Re1−C1	2.186(8)	2.205(7)/2.200(5)	2.183(7)	2.206(6)
Re1−C11	2.355(7)	2.371(7)/2.376(5)	2.355(7)	2.380(6)
C1−P1	1.806(8)	1.782(7)/1.788(1)	1.794(8)	1.797(6)
sum of all bond lengths in the ring	10.647	10.547/10.547	10.553	10.608
Pd1−X1[a]	2.353(2)	2.130(5)/2.133(4)	2.5414(9)	2.5014(8)
Pd1−X2[b]	2.4910(11)	2.129(5)/2.126(4)	2.5327(9)	2.124(6)
Pd1−Pd3	–	2.9434(8)/2.9452(5)	–	–
Pd2−Pd3	–	2.9292(8)/2.9330(5)	–	–
Pd1-P1-C1	113.5(3)	112.9(3)/112.89(19)	113.1(3)	113.2(2)
P1-C1-Re1	110.5(4)	109.0(3)/108.8(3)	109.4(4)	109.5(3)
C1-Re1-C11	82.6(3)	81.8(2)/81.92(19)	82.2(3)	80.7(2)
Re1-C11-Pd1	128.9(3)	127.6(3)/127.5(2)	128.2(4)	129.1(3)
C11-Pd1-P1	84.0(2)	82.8(2)/83.14(15)	83.5(2)	83.65(19)
P1-Pd1-X1[a]	169.44(7)	174.21(14)/174.08(11)	174.19(6)	172.89(5)
P1-Pd1-X2[b]	93.09(6)	94.88(14)/94.70(11)	98.13(6)	96.56(16)
X1-Pd1-X2[a,b]	93.63(6)	89.13(18)/89.41(15)	87.16(3)	90.54(16)
C11-Pd1-X1[a]	88.5(2)	92.9(2)/92.51(18)	91.4(2)	83.65(19)
C11-Pd1-X2[b]	174.1(2)	175.6(2)/176.13(18)	174.7(2)	174.8(3)
Pd1-X1-Pd2	–	–	92.74(3)	–
Pd1-Pd3-Pd2	–	177.73(3)/177.46(2)	–	–
plane(Pd1a-Pd1-Br1)-plane(Pd1a-Pd1-Br1a)	–	–	3.3	–

[a] X1 = atom *trans* to phosphorus in the ring. [b] X2 = atom *cis* to phosphorus in the ring.

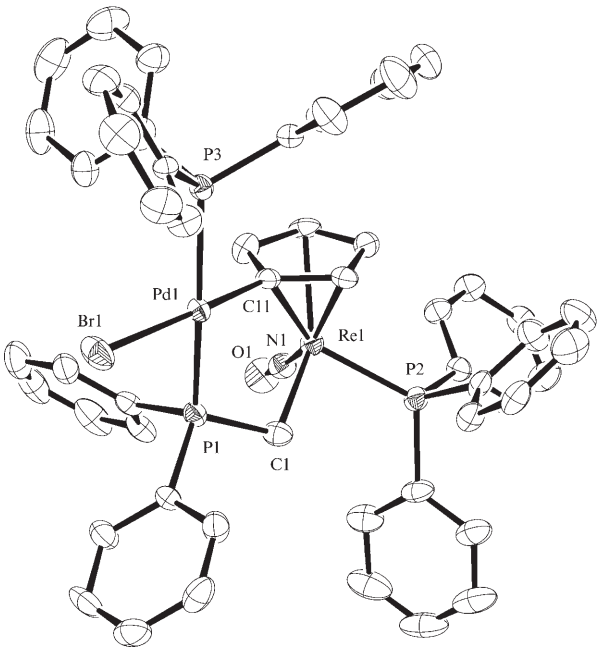

Figure 2. Molecular structure of *SP*-4-4 **11b**·2CH_2Cl_2 with solvate molecules omitted.

tained from (*S*)-**12**$^+$ BF_4^-, the weaker base KOAc, and Pd(OAc)$_2$. However, microanalyses and certain mass spectral peaks were not consistent with an acetate-bridged dimer, and the integrals for the acetate ^{1}H NMR signals did not fit.

Crystals of a solvate were obtained, and the structure was solved analogously to the others above. Interestingly, a *tri*palladium complex, (*S*,*S*)-**13** (Figure 3), had in fact been isolated (71–90% yields). Key bond lengths and angles are summarized in Table 2, and the configurations correspond to retention at rhenium. The crystal structure of the enantiomer (*R*,*R*)-**13** was also determined. Since this constitutes an independent determination of all metrical parameters, data are also included in Table 2.

The tripalladium complex (*S*,*S*)-**13** features an S-shaped $Pd_3(OAc)_4$ core (Figure 3, bottom view). Despite the very large number of molecules that have been palladated by Pd(OAc)$_2$, such moieties are extremely rare (see the Discussion section).[4f,24,25] The three palladium atoms are approximately linear ($\sphericalangle$ 177.46(2)°), with distances (2.9434(8) and 2.9292(8) Å) between those in four other crystallographically characterized examples (range: 3.0457(5) Å[4f] to 2.864(1) Å[24a]). As analyzed elsewhere, these are considered to be outside the bonding range.[4f,26] An idealized C_2 axis passes through the central palladium (perpendicular to the plane of the paper in the bottom view). In this perspective, the palladium-bound PPh_2 (and cyclopentadienyl) units appear *syn*.[27]

We wondered whether other reactant stoichiometries would also give the tripalladium complex (*S*,*S*)-**13**. Isolated (*S*)-**2** and Pd(OAc)$_2$ were combined in a 1.0:0.5 ratio in C_6D_6 (Scheme 5). A new species was detected by NMR spectroscopy (≈81% yield). The ^{1}H NMR spectrum showed signals for one intact cyclopentadienyl ring, and one that had been cyclopalladated (1:1). The ^{31}P NMR spectrum contained two pairs of PPh_3 and CH_2PPh_2 signals. The CH_2PPh_2 signals were coupled, with a value (432 Hz) characteristic of palladium(II) complexes with *trans* phosphine ligands.[28] Hence, the structure shown in Scheme 5, *SP*-4-2 (*S*,*S*)-**14**,[23] is proposed.

When the sample was kept at 80 °C, a second cyclopalladation occurred. The spiropalladacycle (*S*,*S*)-**15** was isolated in 39% yield. Although crystals could be obtained, they were not suitable for X-ray diffraction. Nonetheless, other spiropalladacycles are known,[2c,13] and the structure was supported by many data. For example, the mass spectrum exhibited a strong signal for the molecular ion, and the microanalysis was in excellent agreement. The NMR spectra showed only one type of ligand on palladium, and character-

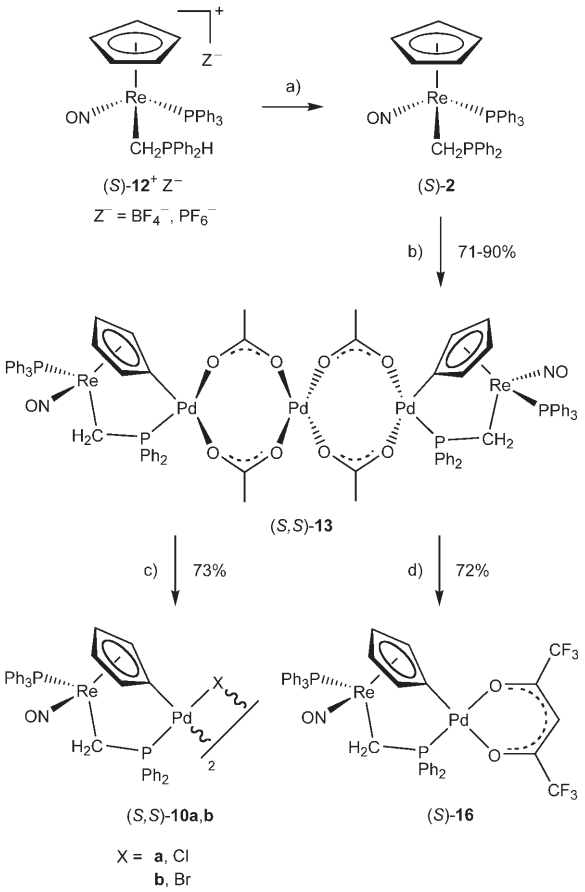

Scheme 4. Syntheses of enantiopure palladacycles from cyclopentadienyl rhenium complexes: a) 1.2 equiv *t*BuOK ($Z^- = PF_6^-$) or KOAc ($Z^- = BF_4^-$), toluene, RT; b) 1.5 equiv $Pd(OAc)_2$, toluene, RT; c) LiX, THF, RT; d) Na(acac-F_6), acetone, RT.

istic chemical shifts for a $(\eta^5\text{-}C_5H_4Pd)Re$ linkage. The ^{13}C NMR signals of the *ortho* carbon atoms of the diastereotopic P*Ph*$_2$ groups gave virtual triplets,[29] consistent with a *trans* stereochemistry. The ^{31}P NMR signals of the PPh_2 and PPh_3 groups were also triplets.

Finally, isolated (*S*)-**2** and $Pd(OAc)_2$ were combined in a 1.0:1.0 ratio in C_6D_6. Analysis by ^{31}P NMR showed that (*S*)-**2** had been consumed, with (*S*,*S*)-**13** constituting ≈61% of the phosphorus-containing products. Several other signals were detected, but no species was present in more than 6% yield. Hence, acetate-bridged palladacycles with 1:1 or 2:2 Re/Pd ratios do not form readily.

Palladacycles from palladacycles: Since the central palladium in (*S*,*S*)-**13** might serve as a source of catalytically active $Pd(OAc)_2$, we sought to remove it. In one approach, the hexafluoroacetylacetonate salt Na(acac-F_6) was added (Scheme 4, bottom right). Workup gave the monopalladium complex (*S*)-**16** (72%). In another approach, the halide salts LiCl and LiBr were added (Scheme 4, bottom left). Workups gave the chloride- and bromide-bridged dipalladium complexes (*S*,*S*)-**10a** (73%) and (*S*,*S*)-**10b** (73%) as 35:65 and 25:75 mixtures of *syn*/*anti* isomers. Crystals of (*S*,*S*)-**10b** were obtained, and the structure was solved analogously to the others above (Figure 4). Only the *anti* isomer crystallized. The Pd_2Br_2 core was nearly planar, with the two $PdBr_2$ planes defining an angle of 3.3°. A C_2 symmetry axis passes through the midpoint.

Complex (*S*,*S*)-**10b** reacted with a variety of neutral two-electron donor ligands (L) to give monopalladium complexes, (*S*)-[$(\eta^5\text{-}C_5H_4)Re(NO)(PPh_3)(\mu\text{-}CH_2PPh_2)Pd(L)(Br)$]. The product (*S*)-**17b**, with L = pyridine (Scheme 6), crystallized in 72% yield.

An X-ray structure (Figure 5) showed the bromide ligand to be *trans* to the CH_2PPh_2 ligand, corresponding to an *SP*-4-2 isomer.[23] In the related complex *SP*-4-4 **11b** (Figure 2), the bromide ligand is *trans* to the cyclopentadienyl ligand, and *cis* to both phosphorus donor ligands. However, NMR spectra of (*S*)-**17b** showed signals for a second geometric isomer (≈67:33), as well as an equilibrium with (*S*,*S*)-**10b** and pyridine.

The reaction of (*S*,*S*)-**10b** and excess 2,4,6-trimethylpyridine gave an adduct analogous to (*S*)-**17b**, as assayed by ^{31}P NMR spectroscopy. A similar reaction of (*S*,*S*)-**10b** and excess PPh_3 showed complete conversion to *SP*-4-4 (*S*)-**11b**, the racemate of which was synthesized according to Scheme 2. Finally, (*S*,*S*)-**13** and PPh_3 (10 equiv) were combined in an NMR tube. The ^{31}P NMR spectrum suggested the formation of a PPh_3 analogue of *SP*-4-2 (*S*,*S*)-**14**.

Catalysis: Suzuki–Miyaura couplings using racemic **10b** as the catalyst precursor were screened under conditions similar to those developed by Buchwald[30] and employed for previous papers in this series.[9] However, because of the exceptional activities, much lower catalyst loadings could be used. As summarized in Table 3, entries 1 and 3–5, $PhB(OH)_2$ (1.5 equiv), the boron-activating base K_3PO_4 (2.0 equiv), an aryl bromide (1.0 equiv), an internal standard, and **10b** (0.01 mol%) were combined in toluene. Couplings proceeded smoothly over the course of 2–55 h at 80°C, giving the expected biaryls in 86–91% yields as analyzed by GC.

Two additional couplings were conducted with 0.001 mol% catalyst loadings (Table 3, entries 2, 6). These also proceeded to completion, although longer reaction times were required. The turnover numbers were very close to 100000, and the yields were slightly higher (96–99%).

Next, (*S*,*S*)-**10b** was evaluated as a catalyst precursor for Mizoroki–Heck couplings of methyl acrylate and 4-bromoacetophenone, 4-iodotoluene, and iodobenzene. Reactions were carried out using 0.36–0.59 mmol% loadings in DMF at 140°C in the presence of NaOAc, $(n\text{Bu})_4N^+Br^-$, and an internal standard, as summarized in the Supporting Information and our previous communication.[10] After 48 h, consumption of the aryl halides was >92%, and the corresponding methyl cinnamate derivatives had formed in 64–76% yields. The turnover numbers were 64100–91400. Reactions with (*S*)-**16** gave comparable data.

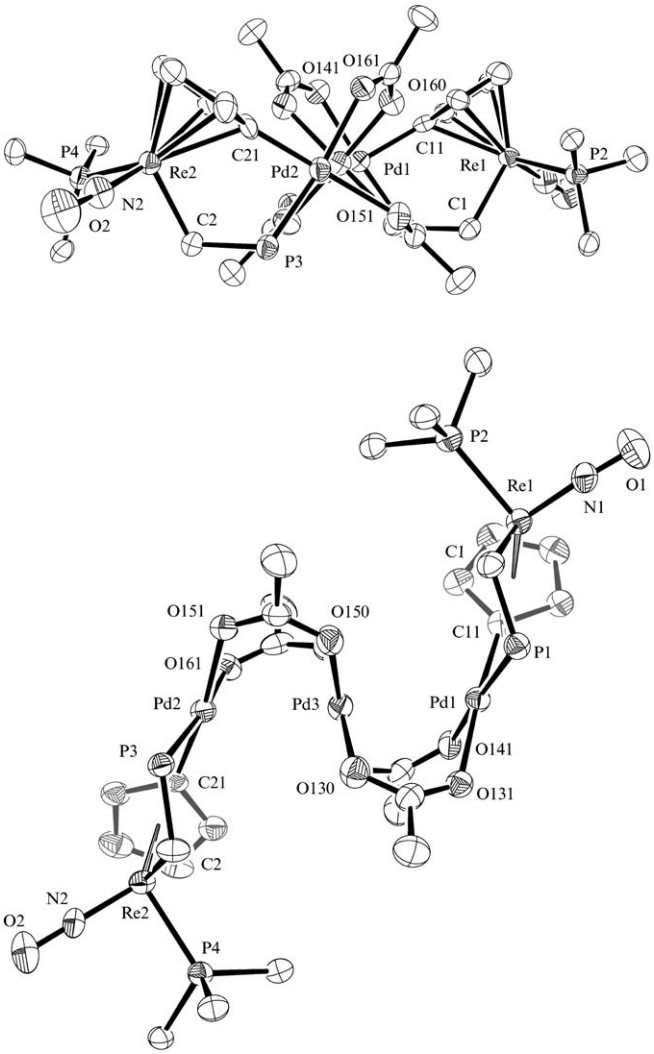

Figure 3. Molecular structure of (*S*,*S*)-**13**·2 C_7H_8 with solvate molecules and PPh_2 and *o*,*m*,*p*-PPh_3 carbon atoms omitted.

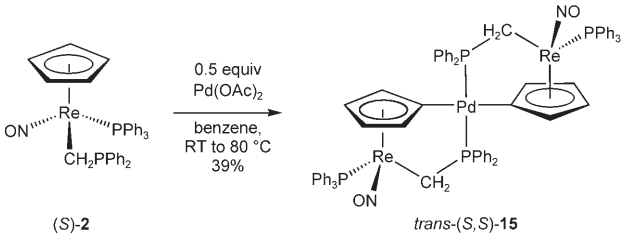

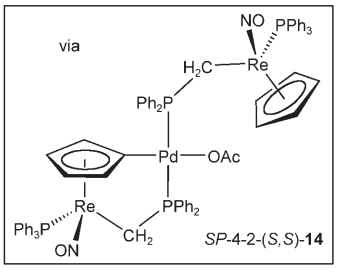

Scheme 5. Other cyclopalladation modes of (*S*)-**2**.

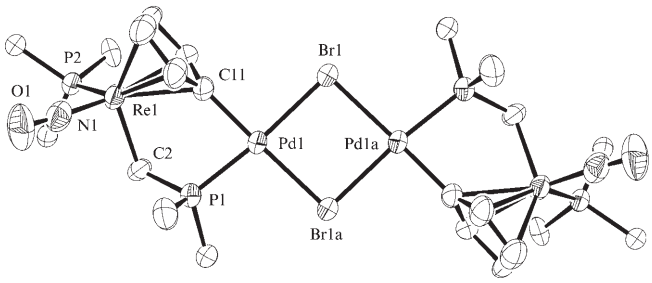

Figure 4. Molecular structure of *anti*-(*S*,*S*)-**10b**·CH_2Cl_2·2 $CHCl_3$ with solvate molecules and *o*,*m*,*p*-PPh_2 and *o*,*m*,*p*-PPh_3 carbon atoms omitted.

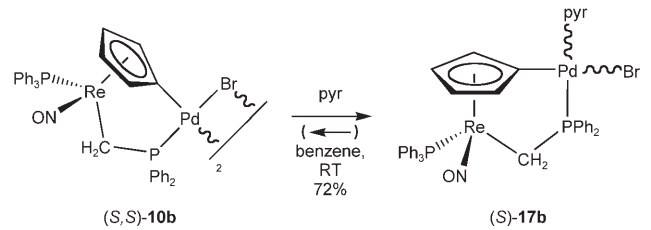

Scheme 6. Synthesis of a monopalladacyclic pyridine complex.

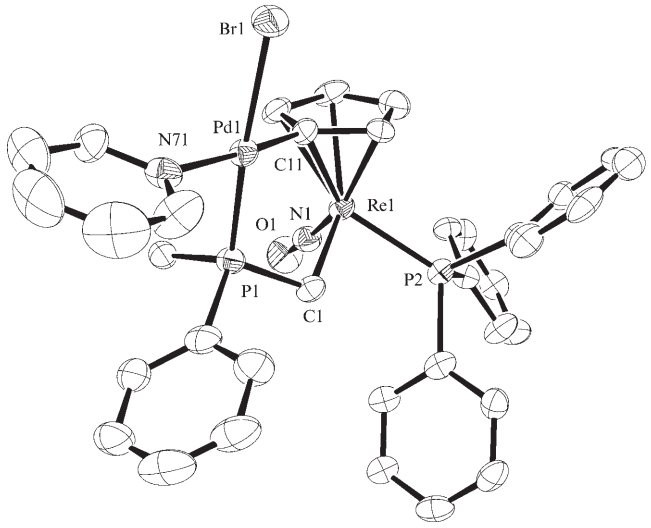

Figure 5. Molecular structure of *SP*-4-2 **17b**·$CHCl_3$ with solvate molecules and *o*,*m*,*p*-PPh_2 carbon atoms for one phenyl omitted.

However, TEM measurements showed the formation of colloidal palladium nanoparticles. A representative result is shown in Figure 6. Similar phenomena have been noted with other "high turnover" Mizoroki–Heck catalysts,[2,3,31,32] especially in recipes that involve $(n\mathrm{Bu})_4\mathrm{N}^+\mathrm{Br}^-$.[31a] Complex (*S*,*S*)-**10b** was also evaluated in Mizoroki–Heck reactions that operate at lower temperatures and yield chiral products,[33] but racemates were always obtained, as detailed elsewhere.[34] Together, these observations suggest that the active catalyst is either nonmolecular or a low-coordinate non-palladacyclic palladium(0) species.[2a,31,32]

Table 3. Suzuki–Miyaura reactions using the racemic palladacycle catalyst precursor **10b**.[a]

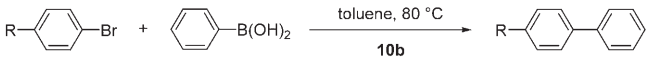

Entry	R	[ArBr]/[Pd][b]	*t* [h]	Conversion[c] [%]	Yield[c] [%]	TON[b,d]
1	H	10000	55	93	91	9100
2[e]	H	100000	96	98	96	96350
3	CH_3	10000	32	93	91	9100
4	CH_3O	10000	32	88	86	8600
5	CH_3CO	10000	2	96	89	8900
6[e]	CH_3O	100000	76	99	99	99780

[a] Conditions: ArBr (1.000 mmol), $PhB(OH)_2$ (1.50 mmol), K_3PO_4 (2.00 mmol), toluene (4.00 mL). [b] Normalized for the number of palladium atoms in **10b**. [c] Conversion of the aryl hydride and yield of the biaryl product were determined by GC using tridecane as internal standard. [d] Based on the product yield. [e] Conducted on a 10.00 mmol scale (ArBr). Catalyst was added as a 0.050 mM solution in toluene.

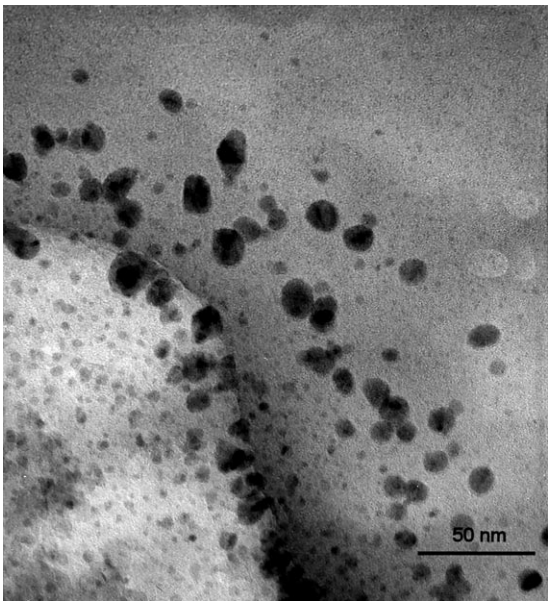

Figure 6. Transmission electron microscopy (TEM) image taken from the Mizoroki–Heck reaction of methyl acrylate and 4-iodotoluene using (*S*)-**16** (see Supporting Information).

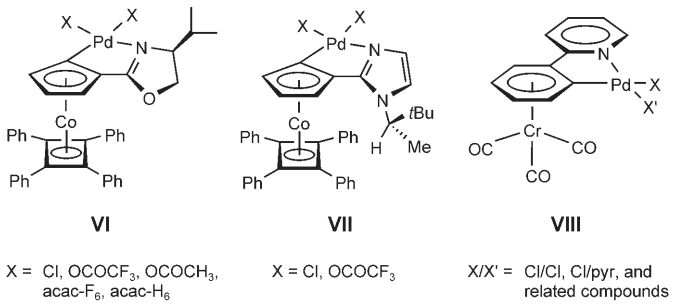

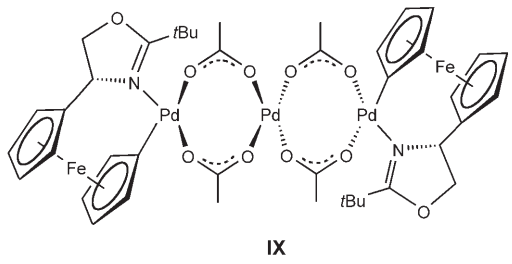

Scheme 7. Previously synthesized palladacycles that contain nonferrocenyl transition metal fragments (top) or a $Pd_3(OAc)_4$ core (bottom).

Discussion

Syntheses of palladacycles: To our knowledge, the new rhenium-containing palladacycles described in Schemes 2–6 are without precedent. Furthermore, there is every reason to assume that these syntheses can be extended to a variety of other metals, donor groups, and ancillary ligands as generalized in Scheme 1. Building blocks of the **IV** type are perhaps even more accessible than **I** and **II**. For example, halides of $[(\eta^5\text{-}C_5Me_5)Fe(L)_2(X)]$ or $[(\eta^5\text{-}C_5Me_5)Mo(L)_3(X)]$, or related thiolates, are easily prepared. Investigations involving such compounds will be described in future publications.

As noted above, a large number ferrocene-containing palladacycles have been reported,[4,11] many of which are chiral and have been isolated in enantiomerically pure form. However, the scarcity of palladacycles that contain other types of metal fragments is striking. Current examples are restricted to cobalt (**VI**, **VII**)[5,12] and chromium (**VIII**) (Scheme 7, top).[13] In contrast to our complexes, in which the rhenium is part of the palladacycle backbone, the metals in **VI**–**VIII** can be viewed as exocyclic substituents. This further reflects the tremendous architectural diversity that can be realized with metal-containing building blocks. A few palladacycles in which ferrocenes are part of the backbone have also been reported.[4f,11f]

Rhenium-containing palladacycles are equally available via insertions into carbon–halogen bonds (Schemes 2, 3) and carbon–hydrogen bonds (Schemes 4, 5). However, formation of the tripalladium tetraacetate complex (*S*,*S*)-**13** was very unexpected. To our knowledge, only three other molecules with such $Pd_3(OAc)_4$ cores have been characterized crystallographically.[4f,24] One (**IX**; Scheme 7, bottom) was obtained recently from an analogous cyclopalladation. However, there is good support from spectroscopic data for several other such complexes.[25]

The bridging acetate ligands fold the palladium square planes essentially on top of each other (Figure 3). In contrast, the Pd_2Br_2 core in (*S*,*S*)-**10b** deviates only slightly from planarity (Figure 4), thereby extending the square planes laterally. The folded $Pd_2(OAc)_2$ linkages may account

for the absence of any detectable acetate-bridged dipalladium complex, as steric interactions between rhenium ligands would be difficult to avoid. Interestingly, the bond lengths and angles associated with the Re–CH_2–P–Pd–C linkages in the crystallographically characterized palladacycles (Table 2) are nearly identical, within experimental error.

Importantly, two other diastereomers of (*S*,*S*)-**13** with identical $Pd_3(OAc)_4$ conformations are possible. These can be termed *anti* (**XI**) and *syn′* (**XII**) (Figure 7). In our opinion, there is no obvious reason why the diastereomer that crystallizes (**X**) should be preferred thermodynamically. However, only a single set of NMR signals is observed, including the ^1H and ^{13}C resonances of the acetate ligands, which should be at least somewhat sensitive to the relative orientations of palladacycles on the termini. Furthermore,

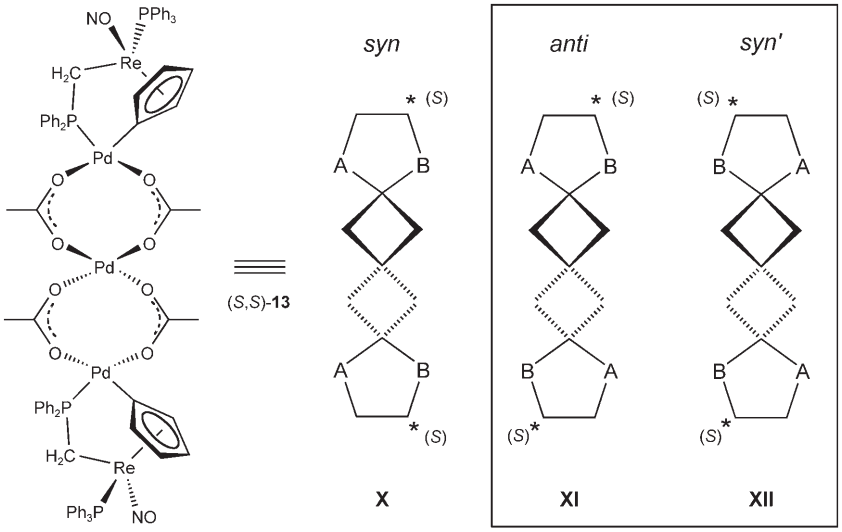

Figure 7. Possible stereoisomers of (*S*,*S*)-**13**.

the acetate ligands *trans* to the cyclopentadienyl and CH_2PPh_2 ligands exhibit distinct ^1H and ^{13}C NMR signals, one of which is coupled to phosphorus. This argues against a rapidly equilibrating mixture of diastereomers.

The chloride-, bromide-, and iodide-bridged palladacycles (*S*,*S*)-**10a**,**b**,**c** exhibit much lower *syn*/*anti* selectivities. Interestingly, the equilibrium ratios become progressively more biased (35:65, 25:75, 21:79). Although it is not possible to rigorously assign the major isomers, the crystal structure of (*S*,*S*)-**10b** suggests that they are *anti*. This crystal structure also shows an absence of steric interactions across the Pd_2Br_2 core, and space-filling models suggest the same for the *syn* isomer. Thus, electronic effects may play a role in the equilibrium ratios.

Catalysis: Like many other palladacycles, those described above are effective catalyst precursors for the Suzuki–Miyaura and Mizoroki–Heck couplings of aryl halides. High turnover numbers can be achieved, although still higher values have been established for other palladacycles.[2,3] However, there are several indications that our palladacycles are not the active catalysts. These include the generation of palladium nanoparticles, as evidenced by TEM (Figure 6), and the formation of racemates in coupling reactions that lead to chiral products.[34] Given the large number of detailed investigations that have established catalysis by nanoparticles or low-coordinate palladium(0) species for related complexes,[31,32] parallel studies were not undertaken.

Nonetheless, there remain several opportunities for future research. For example, according to some models for the formation of low-coordinate palladium(0) species,[2a,35] the spiropalladacycle (*S*,*S*)-**15** would lead to an active catalyst $[\{(\eta^5\text{-}C_5H_4X)Re(NO)(PPh_3)(CH_2PPh_2)\}_nPd]$ ($n = 1$ or 2). In other words, there would be a high probability of chiral supporting ligands, enhancing the prospects for enantioselective catalysis. Furthermore, there are many other types of reactions that are catalyzed by palladacycles,[2] and for which current evidence suggests that the gross structures remain intact. Several of these involve the formation of new stereocenters.[4,5,36]

Also, the extrusion of metal from our palladacycles might prove exploitable. For example, the second metal in **III** or **V** could be engineered to have a labile set of ligands. This might allow the formation under suitable conditions of *bi*metallic colloidal nanoparticles or related nonmolecular species. Such assemblies can be challenging to synthesize, but often exhibit unique and useful properties.[37]

Conclusion

We have established two simple and high-yield routes to a novel new class of palladacycles that contain half-sandwich metal cyclopentadienyl moieties in the backbone (Scheme 1). One involves the reaction of a palladium(0) species with a halocyclopentadienyl complex, and the other the reaction of a palladium(II) species with a cyclopentadienyl complex. Suitable starting materials for the latter route are ubiquitous, and a variety of related syntheses are readily envisioned. Hence, this new methodology should allow the facile and rapid preparation of a very large number of such palladacycles.

Fortuitously, one of our palladacycles is isolated with a rarely occurring $Pd_3(OAc)_4$ core, probably for steric reasons. Although all of these complexes are effective catalyst precursors for common cross-coupling reactions of aryl halides, the available data suggest that either palladium nanoparti-

cles or achiral low-coordinate palladium(0) species are involved. Nonetheless, many other attractive applications for these compounds are easily conceived, and are currently under investigation.

Experimental Section

General: All experiments were carried out under nitrogen unless noted otherwise. NMR spectra were recorded on standard 300–400 MHz FT spectrometers, referenced to the residual solvent signal (δ: ^{1}H: $CHCl_3$, 7.27; C_6D_5H, 7.15; [D_5]acetone, 2.05; ^{13}C: $CDCl_3$, 77.0; C_6D_6, 128.0; [D_6]acetone, 29.9) or H_3PO_4 (δ: ^{31}P, internal capillary, 85%, 0.0), and recorded at 25–28 °C. IR spectra were recorded on an ASI React IR®-1000 spectrometer. Optical rotations were measured as described previously[38] using a Perkin-Elmer model 341 polarimeter. Mass spectra were obtained with a Micromass Zabspec instrument. Gas chromatography was conducted on a ThermoQuest Trace GC 2000 instrument (OPTIMA-5 0.25 μm capillary column, 25 m × 0.32 mm). DSC and TGA data were recorded with a Mettler–Toledo DSC821 instrument and treated by standard methods.[39] Elemental analyses were determined with a Carlo Erba EA1110 CHN instrument. TEM data were recorded on a Philips CM 300 UT microscope.

Chemicals were treated as follows: ether, THF, hexanes, pentane, and toluene, distilled from Na/benzophenone; DMF, benzene, CH_2Cl_2, and $CHCl_3$, distilled from CaH_2; ethyl acetate and acetone, simple distillation; C_6D_6, CD_2Cl_2, $CDCl_3$, and [D_6]acetone (Deutero GmbH), stored over molecular sieves; *n*BuLi (2.5 M in hexanes; Acros), standardized before use;[40] $Ph_3C^+BF_4^-$ (>98%; Fluka) and $Ph_3C^+PF_6^-$ (95.0%; Fluka), stored under argon at −32 °C;[41] pyridine (99.5%; Grüssing), dried over molecular sieves. Other compounds were used as received from common commercial suppliers (Supporting Information).

[(η^5-C_5H_4Br)Re(NO)(CO)$_2$]$^+BF_4^-$ (4b$^+BF_4^-$): A Schlenk flask was charged with [(η^5-C_5H_4Br)Re(CO)$_3$] (**3b**;[16a] 3.461 g, 8.358 mmol) and CH_2Cl_2 (60 mL), and cooled to −15 °C. Then $NO^+BF_4^-$ (1.562 g, 13.373 mmol) was added with stirring. The heterogeneous mixture turned yellow-brown. After 2 h, the cold bath was removed. After 12 h, the solvent was removed by oil-pump vacuum. The residue was extracted with acetone (≈100 mL). The extract was filtered through a plug of Celite (3 cm × 5 cm). The solvent was removed by rotary evaporation. The residue was dried (10^{-3} mbar, 2 h) and washed with THF until the supernatant was colorless (≈2 × 10 mL). The yellow powder was collected by filtration and dried (10^{-3} mbar, 2 h) to give **4b**$^+BF_4^-$ (3.608 g, 7.169 mmol, 86%), decomp 238–240 °C (capillary). Elemental analysis calcd (%) for $C_7H_4BBrF_4NO_3Re$ (503.0): C 16.71, H 0.80, N 2.78; found: C 16.48, H 0.94, N 2.66; ^{1}H NMR (400 MHz, [D_6]acetone): δ = C_5H_4 at 6.96 (t, ^2J(H,H) = 2 Hz, 2H), 6.61 ppm (t, ^2J(H,H) = 2 Hz, 2H); ^{13}C{^{1}H} NMR (101 MHz, [D_6]acetone): δ = 182.1 (s, CO), C_5H_4 at 97.2 (s), 96.5 (s), 96.0 ppm (s); IR (powder film): $\tilde{\nu}$ = 2104 (s, CO), 2042 (s, CO), 1799 (s, NO), 1034 cm^{-1} (s, BF); MS:[42] 416 (100) [**4b**]$^+$.

[(η^5-C_5H_4Br)Re(NO)(PPh$_3$)(CO)]$^+BF_4^-$ (5b$^+BF_4^-$): A Schlenk flask was charged with **4b**$^+BF_4^-$ (3.500 g, 6.958 mmol), CH_2Cl_2 (80 mL), and PPh_3 (5.470 g, 20.88 mmol), and fitted with a condenser. The sample was aspirated with N_2 and refluxed. After 3 h, the mixture was cooled to 0 °C and added to THF (200 mL) with stirring. After 12 h, the precipitate was collected by filtration, washed with THF (3 × 3 mL) and ether (2 × 30 mL), and dried (10^{-3} mbar, 1 h) to give **5**$^+BF_4^-$ as a yellow powder (3.694 g, 5.010 mmol, 72%). Crystallization from CH_2Cl_2/ether gave **5b**$^+BF_4^-$ (3.489 g, 4.732 mmol, 68%) as olive-green needles, decomp 202 °C (capillary). Elemental analysis calcd (%) for $C_{24}H_{19}BBrF_4NO_2PRe$ (737.3): C 39.10, H 2.60, N 1.90; found: C 39.22, H 2.67, N 1.82; ^{1}H NMR (400 MHz, $CDCl_3$): δ = 7.56 (m, 9H of 3C_6H_5), 7.35–7.31 (m, 6H of 3C_6H_5), C_5H_4 at 6.17 (brs, 1H), 6.14 (brs, 1H), 5.83 (brs, 1H), 5.59 ppm (brs, 1H); ^{13}C{^{1}H} NMR (126 MHz, $CDCl_3$): δ = 192.6 (s, CO), PPh_3 at 133.0 (d, ^2J(C,P) = 11 Hz, *o*), 132.6 (d, ^4J(C,P) = 2 Hz, *p*), 129.9 (d, ^1J(C,P) = 61 Hz, *i*), 129.8 (d, ^3J(C,P) = 11 Hz, *m*); C_5H_4 at 96.5 (s), 96.1 (s), 95.4 (s), 94.4 (s), 91.5 ppm (s); ^{31}P{^{1}H} NMR (162 MHz, $CDCl_3$): δ = 11.5 ppm (s, PPh_3); IR (powder film): $\tilde{\nu}$ = 2019 (s, CO), 1760 (s, NO), 1054 cm^{-1} (s, BF); MS:[42] 650 (100) [**5b**]$^+$, 542 (6) [**5b**−Br−CO]$^+$.

[(η^5-C_5H_4Br)Re(NO)(PPh$_3$)(CH$_3$)] (6b): A Schlenk flask was charged with **5b**$^+BF_4^-$ (0.5000 g, 0.6781 mmol) and THF (10 mL). Then $NaBH_4$ (0.0769 g, 2.034 mmol) was added with stirring. After 2 h, the red suspension was filtered through a plug of Celite. The solvent was removed by oil-pump vacuum at room temperature. The residue was extracted with CH_2Cl_2 (≈10 mL). The extract was filtered through SiO_2 (4 × 2 cm) with CH_2Cl_2 rinses. The solvent was removed from the filtrate. The orange residue was dissolved in benzene (≈10 mL) and a layer of hexanes was added gently. After two days, the supernatant was decanted and the red prisms dried (10^{-3} mbar, 2 h) to give **6b**·(C_6H_6)$_{0.5}$ (0.3762 g, 0.5560 mmol, 82%), decomp 136–138 °C (capillary). Elemental analysis calcd (%) for $C_{24}H_{22}BrNOPRe\cdot(C_6H_6)_{0.5}$ (676.6): C 47.93, H 3.72, N 2.07; found: C 47.82, H 3.81, N 2.00; ^{1}H NMR (400 MHz, $CDCl_3$): δ = 7.39–7.35 (m, 3C_6H_5), 7.15 (s, 0.5C_6H_6), C_5H_4 at 5.26 (m, 1H), 4.97 (m, 1H), 4.62 (m, 1H), 4.36 (m, 1H); 1.01 ppm (d, ^3J(H,P) = 6 Hz, CH_3); ^{13}C{^{1}H} NMR (101 MHz, $CDCl_3$): δ = PPh_3 at 135.6 (d, ^1J(C,P) = 52 Hz, *i*), 133.6 (d, ^2J(C,P) = 11 Hz, *o*), 130.1 (d, ^4J(C,P) = 3 Hz, *p*), 128.3 (d, ^3J(C,P) = 10 Hz, *m*); 128.3 (s, C_6H_6), C_5H_4 at 93.7 (s), 89.8 (s), 88.0 (d, ^2J(C,P) = 3 Hz), 87.2 (d, ^2J(C,P) = 3 Hz), 87.1 (s); −28.7 ppm (d, ^2J(C,P) = 7 Hz, CH_3); ^{31}P{^{1}H} NMR (162 MHz, $CDCl_3$): δ = 24.4 ppm (s, PPh_3); IR (powder film): $\tilde{\nu}$ = 1617 cm^{-1} (s, NO); MS:[42] 637 (100) [**6b**]$^+$, 622 (10) [**6b**−CH_3]$^+$, 557 (5) [**6b**−Br]$^+$, 542 (12) [**6b**−Br−CH_3]$^+$.

(*S*)-[(η^5-C_5H_4I)Re(NO)(PPh$_3$)(CH$_3$)] ((*S*)-6c): A Schlenk flask was charged with (*S*)-**8** (0.7313 g, 1.309 mmol)[43] and freshly distilled THF (20 mL), and cooled to −78 °C. Then *n*BuLi (2.6 M in hexanes; 0.504 mL, 1.309 mmol) was added by syringe with stirring. The cold bath was removed. After 1 h, the deep red solution was cooled to −78 °C and solid I_2 (0.3325 g, 1.309 mmol) was added. After 45 min, the cold bath was removed. After a further 1 h, the solvent was removed by oil-pump vacuum. Toluene (4 mL) was added.[44] The suspension was filtered through a plug of SiO_2 (2.5 cm × 6 cm) with toluene rinses under N_2. The orange filtrate was concentrated, and CH_2Cl_2/hexanes (8 mL, 1:1 v/v) was added. The solvents were removed by oil-pump vacuum (5 × 10^{-3} mbar, 1 day) to give (*S*)-**6c** (0.757 g, 1.106 mmol, 84%) as an orange microcrystalline powder, decomp 145 °C (capillary, gradual darkening without melting). Elemental analysis calcd (%) for $C_{24}H_{22}INOPRe$ (684.5): C 42.11, H 3.23, N 2.04; found: C 42.22, H 3.28, N 1.96; $[\alpha]_{21}^{589}$ = +27° ± 3° (*c* = 1.23 mg mL^{-1}, CH_2Cl_2); ^{1}H NMR (400 MHz, C_6D_6): δ = 7.54–7.50 (m, 6H of 3C_6H_5), 7.03–6.94 (m, 9H of 3C_6H_5), C_5H_4 at 4.93 (m, 1H), 4.39 (m, 1H), 4.31 (m, 1H), 4.06 (m, 1H); 1.44 ppm (d, ^3J(H,P) = 6 Hz, 3H, CH_3); ^{13}C{^{1}H} NMR (101 MHz, C_6D_6): δ = PPh_3 at 136.5 (d, ^1J(C,P) = 51 Hz, *i*), 134.0 (d, ^2J(C,P) = 11 Hz, *o*), 130.1 (d, ^4J(C,P) = 2 Hz, *p*);[45] C_5H_4 at 97.5 (s), 94.8 (s), 92.4 (s), 89.6 (s), 47.9 (d, ^2J(C,P) = 4 Hz); −28.7 ppm (d, ^1J(C,P) = 7 Hz, CH_3); ^{31}P{^{1}H} NMR (162 MHz, C_6D_6): δ = 25.7 ppm (s, PPh_3); IR (powder film): $\tilde{\nu}$ = 1625 cm^{-1} (s, NO); MS:[42] 685 (100) [**6c**]$^+$, 557 (6) [**6c**−I]$^+$, 543 (20) [**6c**−I−CH_3]$^+$.

[(η^5-C_5H_4Br)Re(NO)(PPh$_3$)(CH$_2$PPh$_2$H)]$^+BF_4^-$ (7b$^+BF_4^-$): A Schlenk flask was charged with **6b**·(C_6H_6)$_{0.5}$ (0.150 g, 0.222 mmol) and CH_2Cl_2 (10 mL), and was cooled to −60 °C. Then $Ph_3C^+BF_4^-$ (0.0805 g, 0.244 mmol) was added with stirring. After 30 min, PPh_2H (0.0454 g, 0.244 mmol)[46] was added to the light yellow solution. After 10 min, the cold bath was removed. The solution turned orange. After a further 1.5 h, the sample was concentrated (to ≈3 mL) by oil-pump vacuum. The solution was layered with hexanes (20 mL). After 24 h, the orange-red prisms were collected by filtration, washed with pentane (2 × 3 mL), and dried (10^{-3} mbar, 15 min) to give **7b**$^+BF_4^-CH_2Cl_2$ (0.2073 g, 0.2084 mmol, 94%), m.p. 205 °C (capillary). Elemental analysis calcd (%) for $C_{36}H_{32}BBrF_4NOP_2Re\cdot CH_2Cl_2$ (994.6): C 44.88, H 3.45, N 1.41; found: C 45.04, H 3.59, N 1.36; ^{1}H NMR (300 MHz, CD_2Cl_2): δ = 7.87–7.30 (m, 5C_6H_5), 7.26 (ddd (doublet of doublet of doublets), ^1J(H,P) = 492 Hz, ^3J(H,H) = 10 Hz, ^3J(H,H′) = 6 Hz, HP), C_5H_4 at 5.49 (m, 1H), 5.38 (m, 1H), 4.49 (m, 1H), 4.41 (m, 1H); 5.31 (s, CH_2Cl_2), 2.65 (m, C*H*H′), 2.11 ppm (m, CH*H*′); ^{13}C{^{1}H} NMR (101 MHz, CD_2Cl_2): δ = PPh_3 at 134.3 (d, ^1J(C,P) = 52 Hz, *i*), 133.8 (d, ^2J(C,P) = 11 Hz, *o*), 131.6 (s, *p*), 129.5 (d, ^3J(C,P) = 11 Hz, *m*); PPhPh′ at 134.6 (s, *p*), 134.2 (s, *p*′), 132.5 (d, ^2J(C,P) = 10 Hz, *o*), 132.2 (d, ^2J(C,P) = 10 Hz, *o*′), 130.3 (d, ^3J(C,P)

= 12 Hz, *m*), 130.1 (d, ^3J(C,P) = 12 Hz, *m′*), 123.5 (d, ^1J(C,P) = 51 Hz, *i*), 122.3 (d, ^1J(C,P) = 65 Hz, *i′*); C_5H_4 at 93.7 (s), 91.1 (s), 90.9 (s), 90.0 (s), 87.5 (s); 53.5 (s, CH_2Cl_2), −27.4 ppm (d, ^1J(C,P) = 30 Hz, CH_2); $^{31}P\{^1H\}$ NMR (122 MHz, CD_2Cl_2): δ = 31.4 (d, ^3J(P,P) = 13 Hz, PPh_2H), 21.3 ppm (d, ^3J(P,P) = 13 Hz, PPh_3); IR (powder film): $\tilde{\nu}$ = 1660 cm^{-1} (s, NO); MS:[42] 822 (58) $[\mathbf{7b}]^+$, 636 (100) $[\mathbf{7b}-PPh_2H]^+$, 557 (74) $[\mathbf{7b}-PPh_2H\text{-}Br]^+$.

(*S*)-[(η^5-C_5H_4I)Re(NO)(PPh_3)(CH_2PPh_2H)]$^+$ PF_6^- ((*S*)-7c$^+$ PF_6^-): Complex (*S*)-**6c** (0.6033 g, 0.8814 mmol), CH_2Cl_2 (15 mL), Ph_3C^+ PF_6^- (0.3465 g, 0.9695 mmol), and PPh_2H (0.295 g, 1.584 mmol)[46] were combined at −78 °C in a procedure similar to that for **7b**$^+$ BF_4^-. The concentrated sample (≈8 mL) was layered with hexanes (≈25 mL). After 20 h, the supernatant was decanted. The orange prisms were washed with pentane (4×5 mL) and dried by oil-pump vacuum (5×10^{-3} mbar, 1 h) to give (*S*)-**7c**$^+$ PF_6^- (0.885 g, 0.872 mmol, 99 %), decomp 154–156 °C (capillary, gradual darkening without melting). Elemental analysis calcd (%) for $C_{36}H_{32}NOF_6P_3IRe$ (1030.7): C 42.61, H 3.17, N 1.38; found: C 42.70, H 3.21, N 1.44; $[\alpha]_{25}^{589} = -209°\pm5°$ (c = 1.21 mg mL^{-1}, CH_2Cl_2); ^1H NMR (400 MHz, CD_2Cl_2): δ = 7.85–7.32 (m, 25H of $5C_6H_5$); 6.55 (ddd, ^3J-(H,H) = 11.0 Hz, ^3J(H,H′) = 4.8 Hz, HP);[47] C_5H_4 at 5.55 (m, 1H), 5.16 (m, 1H), 4.64 (m, 1H), 4.33 (m, 1H); 2.74–2.64 (m, 1H, C*H*H′), 2.26–2.15 ppm (m, 1H, CH*H*′); $^{13}C\{^1H\}$ NMR (101 MHz, CD_2Cl_2): δ = PPh_3 at 133.8 (d, ^2J(C,P) = 11 Hz, *o*), 133.5 (d, ^1J(C,P) = 59 Hz, *i*), 131.6 (s, *p*), 129.5 (d, ^3J(C,P) = 11 Hz, *m*); PPhPh′ at 134.7 (s, *p*), 134.3 (d, ^4J(C,P) = 4 Hz, *p′*), 132.6 (d, ^2J(C,P) = 9 Hz, *o*), 132.1 (d, ^2J(C,P) = 9 Hz, *o′*), 130.5 (d, ^3J(C,P) = 11 Hz, *m*), 130.1 (d, ^3J(C,P) = 13 Hz, *m′*), 123.7 (d, ^1J(C,P) = 74 Hz, *i*), 122.8 (d, ^1J(C,P) = 83 Hz, *i′*); C_5H_4 at 98.1 (s), 95.1 (s), 93.1 (s), 91.9 (s), 51.8 (s); −24.1 ppm (d, ^1J(C,P) = 28 Hz, CH_2); $^{31}P\{^1H\}$ NMR (162 MHz, CD_2Cl_2): δ = 30.6 (brs, PPh_2), 21.0 (d, ^3J(P,P) = 13 Hz, PPh_3), −143.6 ppm (sep, ^1J(P,F) = 711 Hz, PF_6); IR (powder film): $\tilde{\nu}$ = 1664 cm^{-1} (s, NO); MS:[42] 870 (100) $[\mathbf{7c}+H]^+$, 684 (80) $[\mathbf{7c}-PPh_2H]^+$, 557 (30) $[\mathbf{7c}-CH_2PPh_2H]^+$.

[(η^5-C_5H_4Br)Re(NO)(PPh_3)(CH_2PPh_2)] (1b): A Schlenk tube was charged with **7b**$^+$ BF_4^-·CH_2Cl_2 (0.1520 g, 0.1528 mmol) and THF (10 mL). A solution of *t*BuOK (1.0 M in THF; 0.183 mL, 0.183 mmol) was added with stirring. After 30 min, the solvent was removed by oil-pump vacuum. Benzene (5 mL) was added, and the sample was filtered through a plug of Celite (2 cm×1 cm) with benzene rinses. The filtrate was concentrated (to ≈2 mL) and layered with pentane (15 mL). After 24 h, the supernatant was decanted from orange prisms, which were dried (10^{-3} mbar, 1 h) to give **1b** (0.119 g, 0.145 mmol, 95 %), decomp 165 °C (capillary). Elemental analysis calcd (%) for $C_{36}H_{31}BrNOP_2Re$ (821.7): C 52.62, H 3.80, N 1.70; found: C 52.52, H 3.91, N 1.65; ^1H NMR (400 MHz, C_6D_6): δ = 7.95–7.00 (m, $5C_6H_5$); C_5H_4 at 5.06 (m, 1H), 4.79 (m, 1H), 4.47 (m, 1H), 3.76 (m, 1H); 3.04 (dd, ^2J(H,P) = 12 Hz, ^3J(H,P) = 10 Hz, C*H*H′), 1.96 ppm (dd, ^2J(H,P) = 12 Hz, ^3J(H,P) = 2 Hz, CH*H*′); $^{13}C\{^1H\}$ NMR (101 MHz, C_6D_6): δ = PPh_3 at 135.6 (d, ^1J(C,P) = 52 Hz, *i*), 134.0 (d, ^2J-(C,P) = 11 Hz, *o*), 128.8 (s, *p*), 128.6 (d, ^3J(C,P) = 10 Hz, *m*); PPhPh′ at 147.7 (d, ^1J(C,P) = 24 Hz, *i*), 146.3 (d, ^1J(C,P) = 20 Hz, *i′*), 133.7 (d, ^2J-(C,P) = 18 Hz, *o*), 133.2 (d, ^2J(C,P) = 17 Hz, *o′*), 130.2 (d, ^3J(C,P) = 4 Hz, *m*), 128.8 (d, ^3J(C,P) = 2 Hz, *m′*), 127.7 (s, *p*), 127.4 (s, *p′*); C_5H_4 at 92.7 (t, J(C,P) = 3 Hz), 91.1 (d, J(C,P) = 2 Hz), 88.2 (s), 88.0 (s), 86.9 (s); −11.4 ppm (dd, ^1J(C,P) = 38 Hz, ^3J(C,P) = 6 Hz, CH_2); $^{31}P\{^1H\}$ NMR (162 MHz, C_6D_6): δ = 8.6 (d, ^3J(P,P) = 6 Hz, PPh_2), 26.1 ppm (d, ^3J(P,P) = 6 Hz, PPh_3); IR (powder film): $\tilde{\nu}$ = 1640 cm^{-1} (s, NO); MS:[42] 821 (35) $[\mathbf{1b}]^+$, 637 (100) $[\mathbf{1b}-PPh_2]^+$, 557 (60) $[\mathbf{1b}-PPh_2-Br]^+$.

[(η^5-C_5H_4)Re(NO)(PPh_3)(μ-CH_2PPh_2)Pd(μ-X)]$_2$ (10a, X = Cl; 10b, Br; 10c, I)

Method A: A Schlenk flask was charged with **1b** (0.2785 g, 0.3389 mmol) and toluene (15 mL), and $Pd[P(t\text{Bu})_3]_2$ (0.1732 g, 0.3389 mmol) was added with stirring. The clear yellow solution was stirred at 80 °C. After 5 h, the deep orange solution was concentrated by oil-pump vacuum (to ≈5 mL) and kept at room temperature. After 12 h, the precipitate was collected by filtration, washed with toluene (2×2 mL) and ether (2×10 mL), and dried by oil-pump vacuum (10^{-3} mbar, 2 h) to give **10b**·C_7H_8 (0.2905 g, 0.1491 mmol, 88 %) as a yellow-orange powder. NMR spectra showed mixtures of *syn*/*anti* and *meso*/*rac* diastereomers, decomp 294 °C (capillary). Elemental analysis calcd (%) for $C_{72}H_{62}Br_2N_2O_2P_4Pd_2Re_2\cdot C_7H_8$ (1948.4): C 48.70, H 3.62, N 1.44; found: C 48.62, H 3.47, N 1.37; ^1H NMR (400 MHz, $CDCl_3$): δ = 8.25–8.08 (m, 4H of $11C_6H_5$), 7.50–7.07 (m, 51H of $11C_6H_5$); $2C_5H_4$ at 5.45 (brs, 2H), 5.19/5.14 (2×brs, 69:31,[48] 2H), 4.84/4.76 (2×brs, 69:31,[48] 2H), 2.98/2.89/2.82 (3×brs, 2H); 2.89–2.80 (m, 2C*H*H′), 2.37 ($C_6H_5CH_3$), 2.19–2.03 ppm (m, 2CH*H*′); $^{31}P\{^1H\}$ NMR (162 MHz, $CDCl_3$): δ = 71.5/70.7/70.6/70.4 (4×d, ^3J(P,P) = 23 Hz, PPh_2, 31:69:31:69), 23.6/23.5/23.4/23.3 ppm (4×d, ^3J(P,P) = 23 Hz, PPh_3, 31:69:69:31); IR (powder film): $\tilde{\nu}$ = 1625 cm^{-1} (s, NO); MS:[42] 1856 (32) $[\mathbf{10b}]^+$, 928 (22) $[(\eta^5\text{-}C_5H_4)Re(NO)(PPh_3)(CH_2PPh_2)Pd(Br)]^+$, 848 (70) $[(\eta^5\text{-}C_5H_4)Re(NO)(PPh_3)(CH_2PPh_2)Pd]^+$, 742 (100) $[(\eta^5\text{-}C_5H_4)Re(NO)(PPh_3)(CH_2PPh_2)]^+$.

Method B: A Schlenk flask was charged with (*S*,*S*)-**13**·$2C_7H_8$ (see below; 0.090 g, 0.044 mmol) and LiX (X = Cl, Br; 0.44 mmol), and THF (15 mL) was added with stirring. After 2 h, the red suspension was filtered through a plug of Celite (2.5 cm×4 cm) with THF rinses. The filtrate was taken to dryness by oil-pump vacuum. Then CH_2Cl_2 (2 mL) was added. The red suspension was filtered through a plug of SiO_2 (2.5 cm×4 cm) with CH_2Cl_2. The yellow-orange fractions were concentrated by oil-pump vacuum (to ≈5 mL) and pentane (≈40 mL) was added. After 24 h, the supernatant was decanted carefully from the precipitate, which was dried by oil-pump vacuum (5×10^{-3} mbar, 1 day) to give (*S*,*S*)-**10** as a bright yellow powder ((*S*,*S*)-**10a**, 0.060 g, 0.032 mmol, 73 %; (*S*,*S*)-**10b**, 0.056 g, 0.032 mmol, 73 %). NMR spectra showed mixtures of *syn*/*anti* isomers.

(*S*,*S*)-10a: Elemental analysis calcd (%) for $C_{72}H_{62}Cl_2N_2O_2P_4Pd_2Re_2$ (1767.3): C 48.93, H 3.54, N 1.59; found: C 48.62, H 3.62, N 1.58; $[\alpha]_{26}^{589} = -138°\pm8°$ (c = 1.05 mg mL^{-1}, THF); ^1H NMR (400 MHz, $CDCl_3$): δ = 8.31–7.01 (m, $10C_6H_5$), $2C_5H_4$ at 5.45 (brs, 2H), 5.18 (d, J(H,H) = 2 Hz, 2H), 4.86 (brs, 2H), 2.97/2.83 (2×brs, minor/major isomer, 2H); 2.83–2.71 (m, 2H, 2C*H*H′), 2.20–2.01 ppm (m, 2H, 2CH*H*′); $^{13}C\{^1H\}$ NMR (101 MHz, $CDCl_3$, partial data): δ = PPh_3 at 136.0 (d, ^1J(C,P) = 52 Hz, *i*),[49] 134.4 (d, ^2J(C,P) = 10 Hz, *o*),[49] 130.0 (s, *p*),[49] 128.4 (d, ^3J(C,P) = 9 Hz, *m*);[49,50] C_5H_4 (major isomer)[50] at 121.5 (m), 92.4 (m), 90.2 (s), 89.4 (brs), 86.0 (m); CH_2 at −11.3 (m, major isomer), −12.8 ppm (m, minor isomer); $^{31}P\{^1H\}$ NMR (162 MHz, $CDCl_3$): δ = 68.1 (d, ^3J(P,P) = 23 Hz, PPh_2, major isomer, 65 %), 67.4 (d, ^3J(P,P) = 22 Hz, P′Ph_2, minor isomer, 35 %), 23.6 (d, ^3J(P,P) = 22 Hz, P′Ph_3, minor isomer, 35 %), 23.2 ppm (d, ^3J(P,P) = 24 Hz, PPh_3, major isomer, 65 %). IR (powder film): $\tilde{\nu}$ = 1629 cm^{-1} (s, NO); MS:[42] 1766 (15) $[\mathbf{10a}-H]^+$, 883 (40) $[(\eta^5\text{-}C_5H_5)Re(NO)(PPh_3)(CH_2PPh_2)Pd(Cl)]^+$, 848 (60) $[(\eta^5\text{-}C_5H_5)Re(NO)(PPh_3)(CH_2PPh_2)Pd]^+$, 742 (100) $[(\eta^5\text{-}C_5H_4)Re(NO)(PPh_3)(CH_2PPh_2)]^+$.

(*S*,*S*)-10b: DSC: exotherm T_i 232.2 °C, T_e 249.3 °C, T_p 261.2 °C, T_c 271.3 °C, T_f 295.9 °C; TGA: onset of mass loss, T_i 254.3 °C. Elemental analysis (%) calcd for $C_{72}H_{62}Br_2N_2O_2P_4Pd_2Re_2$ (1856.25): C 46.59, H 3.37, N 1.51; found: C 46.54, H 3.44, N 1.51; ^1H NMR (400 MHz, $CDCl_3$): δ = 8.27–7.08 (m, $10C_6H_5$), $2C_5H_4$ at 5.46 (brs, 2H), 5.18 (brs, 2H), 4.84 (brs, 2H), 2.98/2.84 (2×brs, minor/major isomer, 2H); 2.88–2.79 (m, 2H, 2C*H*H′), 2.19–2.03 ppm (m, 2H, 2CH*H*′); $^{13}C\{^1H\}$ NMR (101 MHz, $CDCl_3$): δ = PPh_3 at 136.3 (d, ^1J(C,P) = 51 Hz, *i*),[49] 134.4 (d, ^2J(C,P) = 10 Hz, *o*),[49] 130.0 (s, *p*),[49] 128.3 (d, ^3J(C,P) = 10 Hz, *m*);[49] PPhPh′ (major isomer) at 141.8 (d, ^1J(C,P) = 29 Hz, *i*), 134.9 (d, ^2J(C,P) = 11 Hz, *o*), 134.6 (d, ^2J(C,P) = 11 Hz, *o′*), 131.3 (s, *p*), 131.2 (s, *p′*), 127.5 (d, ^3J(C,P) = 10 Hz, *m*); PPhPh′ (minor isomer) at 132.1 (d, ^2J(C,P) = 11 Hz, *o*), 130.5 (s, p), 129.1 (s, *p′*);[45,50] C_5H_4 (major isomer)[49,50] at 123.9 (m), 92.5 (m), 90.2 (s), 89.5 (s), 85.9 (s); −10.8 ppm (brd, ^1J(C,P) = 16 Hz, CH_2);[49] $^{31}P\{^1H\}$ NMR (162 MHz, $CDCl_3$): δ = 70.9 (d, ^3J(P,P) = 23 Hz, PPh_2, major isomer, partial overlap), 70.7 (d, ^3J(P,P) = 20 Hz, P′Ph_2, minor isomer, partial overlap), 23.9 (d, ^3J(P,P) = 22 Hz, P′Ph_3, minor isomer, ≈25 %), 23.6 ppm (d, ^3J(P,P) = 24 Hz, PPh_3, major isomer, ≈75 %); IR (powder film): $\tilde{\nu}$ = 1629 cm^{-1} (s, NO); MS:[42] 1856 (15) $[\mathbf{10b}]^+$, 1035 (5) $[(\eta^5\text{-}C_5H_4)Re(NO)(PPh_3)(CH_2PPh_2)Pd(Br)Pd]^+$, 928 (18) $[(\eta^5\text{-}C_5H_4)Re(NO)(PPh_3)(CH_2PPh_2)Pd(Br)]^+$, 848 (22) $[(\eta^5\text{-}C_5H_4)Re(NO)(PPh_3)(CH_2PPh_2)Pd]^+$, 742 (100) $[(\eta^5\text{-}C_5H_4)Re(NO)(PPh_3)(CH_2PPh_2)]^+$.

Method C: A Schlenk flask was charged with (*S*)-**7c**$^+$ PF_6^- (0.103 g, 0.1015 mmol),[20b] and toluene (7 mL). Then *t*BuOK (1.0 M in THF; 0.152 mL, 0.152 mmol) was added by syringe with stirring. The mixture

was stirred vigorously to give a yellow suspension. After 2 h, solid Pd[P(*t*Bu)$_3$]$_2$ (0.0519 g, 0.1015 mmol) was added. After a further 20 h, pentane (25 mL) was added to the brown mixture. The yellow precipitate was collected by filtration and washed with pentane (10 mL). A small amount of CH_2Cl_2 was added. The mixture was filtered through a plug of silica (2 cm × 4 cm) with CH_2Cl_2/hexanes (1:1 v/v, ≈20 mL) and then CH_2Cl_2. The latter fractions were yellow, and were concentrated by oil-pump vacuum to ≈2 mL. Then pentane (≈10 mL) was added. After 24 h, the supernatant was carefully decanted from the precipitate, which was dried by oil-pump vacuum (4×10^{-3} mbar, 1 day) to give (*S*,*S*)-**10c** (0.022 g, 0.011 mmol, 22 %)[20b] as a yellow-orange powder. NMR spectra showed mixtures of *syn*/*anti* isomers. Elemental analysis calcd (%) for $C_{72}H_{62}I_2N_2O_2P_4Pd_2Re_2$ (1950.2): C 44.34, H 3.20, N 1.44; found: C 43.23, H 3.16, N 1.33; ^{1}H NMR (400 MHz, $CDCl_3$): δ = 8.22–7.01 (m, 10 C_6H_5),[49] 2 C_5H_4 (major/minor isomer) at 5.44/5.46 (brs/brs, 2H), 5.17/5.20 (d/brs, *J*(H,H) = 2/– Hz, 2H), 4.82/4.82 (brs/brs, 2H), 2.96/2.86 (brs/brs, 2H); 2.93–2.86 (m, 2H, 2C*H*H′), 2.18–2.08 ppm (m, 2H, 2CH*H*′); ^{13}C{^{1}H} NMR (101 MHz, $CDCl_3$): δ = PPh_3 at 136.3 (d, ^1J(C,P) = 51 Hz, *i*),[49] 133.4 (d, ^2J(C,P) = 10 Hz, *o*),[49] 130.0 (s, *p*),[49] 128.3 (d, ^3J(C,P) = 10 Hz, *m*);[49] PPhPh′ (major isomer) at 143.6 (d, ^1J(C,P) = 25 Hz, *i*), 134.7 (d, ^2J(C,P) = 12 Hz, *o*), 131.9 (d, ^1J(C,P) = 57 Hz, *i*′), 131.2 (d, ^2J(C,P) = 10 Hz, *o*′), 130.4 (s, *p*), 129.0 (s, *p*′), 127.7 (d, ^3J(C,P) = 10 Hz, *m*);[45,50] C_5H_4 (major isomer)[49,50] at 126.7 (m), 92.8 (m), 90.6 (s), 90.0 (s), 86.1 (s); –9.7 ppm (m, CH_2);[49] ^{31}P{^{1}H} NMR (162 MHz, $CDCl_3$): δ = 74.9 (d, ^3J(P,P) = 24 Hz, PPh_2, minor isomer, ≈21 %), 70.7 (d, ^3J(P,P) = 24 Hz, P′Ph_2, major isomer, ≈79 %), 23.8 (downfield signal of minor isomer), 23.5 ppm (d, ^3J(P,P) = 25 Hz, PPh_3, major isomer, partial overlap); IR (powder film): $\tilde{\nu}$ = 1633 cm^{-1} (s, NO); MS:[42] 1949 (10) [**10c**–H]$^+$, 975 (10) [(η^5-C_5H_5)Re(NO)(PPh_3)(CH_2PPh_2)Pd(I)]$^+$, 848 (15) [(η^5-C_5H_5)Re(NO)(PPh_3)(CH_2PPh_2)Pd]$^+$, 742 (100) [(η^5-C_5H_4)Re(NO)(PPh_3)(CH_2PPh_2)]$^+$.

***SP*-4-4-[(η^5-$\overline{C_5H_4}$)Re(NO)(PPh_3)(μ-CH_2PPh_2)$\overline{Pd}$(PPh_3)(Br)] (*SP*-4-4 11b)**:[23] A Schlenk tube was charged with **10b**·C_7H_8 (0.1130 g, 0.0580 mmol), CH_2Cl_2 (10 mL), and PPh_3 (0.0912 g, 0.3480 mmol). The suspension was stirred and gradually became a bright yellow solution. After 1 h, the solution was filtered through a plug of Celite (2 cm × 1 cm) with CH_2Cl_2 rinses, concentrated by oil-pump vacuum to ≈3 mL, and layered with hexanes (≈10 mL). After 2 days, the supernatant was decanted. The yellow prisms were washed with small portions of pentane and dried (10^{-3} mbar, 1 h) to give dull yellow chips of *SP*-4-4 **11b** (0.0635 g, 0.0534 mmol, 92 %), m.p. 166–168 °C (capillary). Elemental analysis calcd (%) for $C_{54}H_{46}BrNOP_3PdRe$ (1190.4): C 54.48, H 3.89, N 1.18; found: C 54.70, H 4.13, N 1.19; ^{1}H NMR (400 MHz, $CDCl_3$): δ = 7.56–7.23 (m, 8 C_6H_5), C_5H_4 at 5.06 (brs, 1H), 4.86 (brs, 1H), 4.50 (brs, 1H), 2.32 (brs, 1H); 2.96 (ddd, ^2J(H,P) = 14 Hz, ^2J(H,H) = 7 Hz, ^3J(H,P) = 2 Hz, C*H*H′), 2.33 (ddd, ^2J(H,P) = 31 Hz, ^2J(H,H) = 7 Hz, ^3J(H,P) = 2 Hz, CH*H*′); ^{13}C{^{1}H} NMR (101 MHz, $CDCl_3$): δ = $RePPh_3$ and $PdPPh_3$ at 136.3 (d, ^1J(C,P) = 51 Hz, *i*), 134.9 (d, ^2J(C,P) = 12 Hz, *o*), 133.4 (d, ^2J(C,P) = 11 Hz, *o*′), 131.7 (d, ^1J(C,P) = 37 Hz, *i*′), 129.9 (d, ^2J(C,P) = 2 Hz, *p*), 129.8 (d, ^2J(C,P) = 2 Hz, *p*′), 128.3 (d, ^3J(C,P) = 10 Hz, *m*), 128.0 (d, ^3J(C,P) = 10 Hz, *m*′); PPhPh′ at[51] 134.9 (d, ^1J(C,P) = 41 Hz, *i*), 132.8 (d, ^1J(C,P) = 49 Hz, *i*′), 132.1 (d, ^2J(C,P) = 9 Hz, *o*), 131.6 (d, ^2J(C,P) = 14 Hz, *o*′), 130.3 (s, *p*), 129.0 (s, *p*′), 128.5 (d, ^3J(C,P) = 12 Hz, *m*), 127.4 (d, ^3J(C,P) = 10 Hz, *m*′); C_5H_4 at 143.1 (dd, ^2J(C,P) = 23 Hz, ^2J(C,P) = 8 Hz, PdC), 92.6 (m), 91.4 (d, *J*(C,P) = 6 Hz), 89.2 (s), 85.6 (s); –8.7 ppm (d, ^1J(C,P) = 13 Hz, CH_2); ^{31}P{^{1}H} NMR (162 MHz, $CDCl_3$): δ = 72.1 (dd, ^2J(P,P) = 457 Hz, ^3J(P,P) = 26 Hz, PPh_2), 23.8 (d, ^3J(P,P) = 26 Hz, $RePPh_3$), 19.6 ppm (d, ^2J(P,P) = 457 Hz, $PdPPh_3$); IR (powder film): $\tilde{\nu}$ = 1625 cm^{-1} (s, NO); MS:[42] 1191 (60) [**11b**]$^+$, 1110 (30) [**11b**–Br]$^+$, 929 (25) [**11b**–PPh_3]$^+$, 848 (100) [**11b**–Br–PPh_3]$^+$, 742 (46) [**11b**–Br–PPh_3–Pd]$^+$.

(*S*,*S*)-[(η^5-$\overline{C_5H_4}$)Re(NO)(PPh_3)(μ-CH_2PPh_2)$\overline{Pd}$(μ-OAc)$_2$Pd(μ-OAc)$_2$$\overline{Pd}$(μ-$PPh_2CH_2$)($Ph_3P$)(ON)Re(η^5-$\overline{C_5H_4}$)] ((*S*,*S*)-13)

Method A: A Schlenk flask was charged with (*S*)-**12**$^+$ BF_4^- (0.350 g, 0.421 mmol),[6a] $Pd(OAc)_2$ (0.1419 g, 0.632 mmol), KOAc (0.050 g, 0.505 mmol), and toluene (25 mL). The mixture was stirred for 14 h. The black suspension was filtered through a plug of Celite (2.5 cm × 5 cm) with toluene rinses. The orange filtrate (65 mL) was layered gently with pentane (280 mL). After 72 h, the supernatant was decanted and the orange-red crystals were dried under a N_2 stream to give (*S*,*S*)-**13**·2 C_7H_8 (0.331 g, 0.149 mmol, 71 %), decomp 155 °C (capillary, gradual darkening without melting). DSC: endotherm, T_i 137.5 °C, T_e 154.0 °C, T_p 181.1 °C, T_c 196.7 °C, T_f 196.7 °C; endotherm, T_i 196.9 °C, T_e 199.0 °C, T_p 202.8 °C, T_c 205.8 °C, T_f 205.9 °C; TGA: onset of first mass loss regime, T_i 123.5 °C, T_f 175.6 °C (6.5 % mass loss; theory for 2 C_7H_8 8.2 %), onset of second mass loss regime, T_i 176.0 °C, T_f 266.6 °C. Elemental analysis calcd (%) for $C_{80}H_{74}N_2O_{10}P_4Pd_3Re_2$·2 C_7H_8 (2223.16): C 50.78, H 4.08, N 1.26; found: C 50.75, H 4.13, N 1.28; $[\alpha]_{26}^{589}$ = –314° ± 4° (*c* = 0.91 mg mL^{-1}, THF); ^{1}H NMR (400 MHz, C_6D_6): δ = 8.73–8.68 (m, 4H of 12 C_6H_5), 7.64–7.59 (m, 4H of 12 C_6H_5), 7.45–6.87 (m, 52H of 12 C_6H_5), 2 C_5H_4 at 5.54 (brs, 2H), 5.13 (brs, 2H), 4.82 (m, 2H), 4.78 (brs, 2H); 3.50 (m, 2H, 2C*H*H′), 2.10 (s, 6H, 2 $C_6H_5CH_3$), 2.07 (m, 2H, 2CH*H*′), 1.58 (s, 6H, 2 Ac), 1.49 ppm (s, 6H, 2 Ac′); ^{13}C{^{1}H} NMR (101 MHz, C_6D_6): δ = 182.4 (s, C=O), 182.2 (s, C′=O), PPh_3 at 136.8 (d, ^1J(C,P) = 51 Hz, *i*), 134.1 (d, ^2J(C,P) = 10 Hz, *o*), 130.0 (s, *p*);[45] PPhPh′ at 143.2 (d, ^1J(C,P) = 25 Hz, *i*), 135.1 (d, ^2J(C,P) = 10 Hz, *o*), 133.5 (d, ^1J(C,P) = 62 Hz, *i*′), 131.8 (d, ^2J(C,P) = 9 Hz, *o*′), 130.6 (s, *p*), 128.7 (s, *p*′);[45] C_5H_4 at 120.0 (s), 95.8 (m), 90.6 (s), 87.4 (s), 86.6 (s); 23.9 (d, ^4J(C,P) = 5 Hz, CCH_3),[52] 23.4 (s, CC′H_3), –13.3 (d, ^1J(C,P) = 20 Hz, CH_2); $C_6H_5CH_3$ at 137.8 (s, *i*), 129.3 (s, *o*), 128.5 (s, *m*), 125.7 (s, *p*), 21.6 ppm (s, CH_3); ^{31}P{^{1}H} NMR (162 MHz, C_6D_6): δ = 61.3 (d, ^3J(P,P) = 25 Hz, PPh_2), 25.3 ppm (d, ^3J(P,P) = 25 Hz, PPh_3); IR (powder film): $\tilde{\nu}$ = 1633 (s, NO), 1559 (vs, CO), 1401 cm^{-1} (s, CO); MS:[42] 2040 (6) [**13**]$^+$, 1979 (2) [**13**–OAc]$^+$, 1014 (9) [(η^5-C_5H_4)Re(NO)(PPh_3)(CH_2PPh_2)Pd_2(OAc)]$^+$, 907 (100) [(η^5-C_5H_4)Re(NO)(PPh_3)(CH_2PPh_2)Pd(OAc)]$^+$, 848 (6) [(η^5-C_5H_4)Re(NO)(PPh_3)(CH_2PPh_2)Pd]$^+$, 742 (12) [(η^5-C_5H_4)Re(NO)(PPh_3)(CH_2PPh_2)]$^+$.

Method B: A Schlenk flask was charged with (*S*)-**12**$^+$ PF_6^- (0.800 g, 0.900 mmol),[53] $Pd(OAc)_2$ (0.303 g, 1.35 mmol), and toluene (50 mL). Then *t*BuOK (1.0 M in THF; 1.35 mL, 1.35 mmol) was added by syringe with stirring. The yellow mixture turned dark brown. After 14 h, the solvent was removed by oil-pump vacuum and the brown-black residue was suspended in a small amount of ethyl acetate. This was filtered through a plug of SiO_2 (2.5 cm × 18 cm) using ethyl acetate/pentane (1:1 v/v). The orange fractions were concentrated to ≈15 mL. Then pentane (60 mL) was added. The yellow powder was collected by filtration, washed with pentane (2 × 20 mL), and dried by oil-pump vacuum (5×10^{-3} mbar, 2 days) to give (*S*,*S*)-**13** (0.826 g, 0.405 mmol, 90 %) as a yellow powder, decomp 199 °C (capillary, gradual darkening without melting); TGA: onset of mass loss, T_i 176.0 °C. Elemental analysis (%) calcd for $C_{80}H_{74}N_2O_{10}P_4Pd_3Re_2$ (2039.04): C 47.12, H 3.66, N 1.37; found: C 47.12, H 3.69, N 1.47. The ^{1}H and ^{13}C NMR spectra were identical to those of (*S*,*S*)-**13**·2 C_7H_8, except for the absence of solvate peaks; IR (powder film): $\tilde{\nu}$ = 1637 (s, NO), 1563 (vs, CO), 1401 cm^{-1} (s, CO); MS:[42] 2040 (6) [**13**]$^+$, 1980 (4) [**13**–OAc]$^+$, 1014 (12) [(η^5-C_5H_5)Re(NO)(PPh_3)(CH_2PPh_2)Pd_2(OAc)]$^+$, 908 (100) [(η^5-C_5H_5)Re(NO)(PPh_3)(CH_2PPh_2)Pd(OAc)]$^+$.

***SP*-4-2 (*S*,*S*)-[(η^5-$\overline{C_5H_4}$)Re(NO)(PPh_3)(μ-CH_2PPh_2)$\overline{Pd}$(μ-PPh_2CH_2)(NO)(Ph_3P)Re(η^5-C_5H_5)(η^1-OAc)] (*SP*-4-2 (*S*,*S*)-14)**:[23] An NMR tube was charged with (*S*)-**2**·C_6H_6 (0.025 g, 0.030 mmol)[7a] and $Pd(OAc)_2$ (0.0034 g, 0.015 mmol), and sealed with a septum. Then C_6D_6 (0.6 mL) was added by syringe. After 22 h, ^{1}H and ^{31}P NMR spectra showed *SP*-4-2 (*S*,*S*)-**14** to be the main product (81 %, as assayed by integration of the ^{31}P NMR spectrum). ^{1}H NMR (400 MHz, C_6D_6): δ = 8.70–8.65 (m, 2H of 10 C_6H_5), 7.98–7.93 (m, 2H of 10 C_6H_5), 7.61–7.36 (m, 20H of 10 C_6H_5), 7.36–6.92 (m, 26H of 10 C_6H_5), C_5H_4 at 5.13 (brs, 1H), 4.67 (brs, 1H), 4.64 (brs, 1H), 2.84 (brs, 1H); 5.09 (s, 5H, C_5H_5), 3.26–3.21 (m, 1H, C*H*H′), 2.77–2.67 (m, 1H, CH*H*′), 2.54–2.51 (m, 2H, CH_2″), 2.10 ppm (s, 3H, OAc); ^{31}P{^{1}H} NMR (162 MHz, C_6D_6): δ = 62.8 (dd, ^2J(P,P) = 431 Hz, ^3J(P,P) = 25 Hz, PPh_2), 35.8 (dd, ^2J(P,P) = 432 Hz, ^3J(P,P) = 18 Hz, PPh_2′), 25.5 (d, ^3J(P,P) = 24 Hz, PPh_3), 25.5 ppm (d, ^3J(P,P) = 19 Hz, PPh_3′).

***trans*-(*S*,*S*)-[{(η^5-$\overline{C_5H_4}$)Re(NO)(PPh_3)(μ-CH_2PPh_2)}$_2$$\overline{Pd}$] (*trans*-(*S*,*S*)-15)**: A Schlenk flask was charged with (*S*)-**2**·C_6H_6 (0.1476 g, 0.180 mmol), Pd(OAc)$_2$ (0.0198 g, 0.088 mmol), and toluene (7 mL). The orange solution was stirred for 3.5 days at room temperature and then 1 day at 80 °C. The toluene was removed from the brown-black mixture by oil-pump

vacuum. Then a small amount of CH_2Cl_2 was added. The suspension was filtered through a plug of SiO_2 (2.5 cm × 7 cm) with CH_2Cl_2. The solvent was removed from the yellow fraction by oil-pump vacuum. The residue was dissolved in benzene (5 mL) and layered gently with pentane (20 mL). After 2 days, the supernatant was decanted and the orange crystals dried by oil-pump vacuum (5×10^{-3} mbar, 1 h) to give *trans*-(*S*,*S*)-**15** (0.050 g, 0.032 mmol, 39%), decomp 181–183 °C (capillary, gradual darkening without melting). Elemental analysis calcd (%) for $C_{72}H_{62}N_2O_2P_4PdRe_2$ (1590.0): C 54.38, H 3.93, N 1.76; found: C 54.39, H 3.93, N 1.63; $[\alpha]_{24}^{589} = +53°\pm4°$ (c = 1.16 mg mL^{-1}, THF); ^{1}H NMR (400 MHz, C_6D_6): δ = 8.41–8.37 (m, 4H of 10 C_6H_5), 7.49–7.43 (m, 16H of 10 C_6H_5), 7.28–7.21 (m, 6H of 10 C_6H_5), 6.98–6.92 (m, 18H of 10 C_6H_5), 6.80–6.74 (m, 6H of 10 C_6H_5); 2 C_5H_4 at 5.31 (brs, 2H), 5.05 (brs, 2H), 5.00 (m, 2H), 2.59 (brs, 2H); 3.19–3.14 (m, 2H, 2C*H*H′), 2.85–2.82 ppm (m, 2H, 2CH*H*′); ^{13}C{^{1}H} NMR (101 MHz, C_6D_6): δ = PPh_3 at 137.6 (d, ^1J(C,P) = 49 Hz, *i*), 133.8 (d, ^2J(C,P) = 10 Hz, *o*), 129.6 (s, *p*);[45] PPhPh′ at 136.9 (d, ^2J(C,P) = 23 Hz, *i*), 136.7 (d, ^2J(C,P) = 30 Hz, *i*′), 134.9 (virtual t, ^2J(C,P) = 6 Hz, *o*), 131.4 (virtual t, ^2J(C,P) = 5 Hz, *o*′), 129.6 (s, *p*);[45] C_5H_4 at 143.9 (dd, ^2J(C,P) = 20 Hz, ^2J(C,P) = 11 Hz, Pd*C*) 95.0 (m), 93.2 (s), 91.4 (s), 86.8 (s);[50] −8.7 ppm (brs, CH_2); ^{31}P{^{1}H} NMR (162 MHz, C_6D_6): δ = 65.5 (virtual t, ^3J(P,P) = 14 Hz, PPh_2), 26.5 ppm (virtual t, ^3J(P,P) = 14 Hz, PPh_3); IR (powder film): $\tilde{\nu}$ = 1633 cm^{-1} (s, NO); MS:[42] 1591 (60) [**15**]$^+$, 848 (35) [(η^5-C_5H_4)Re(NO)(PPh_3)-(CH_2PPh_2)Pd]$^+$, 742 (100) [(η^5-C_5H_4)Re(NO)(PPh_3)(CH_2PPh_2)]$^+$.

(*S*)-[(η^5-C_5H_4)Re(NO)(PPh_3)(μ-CH_2PPh_2)Pd(acac-F_6)] ((*S*)-16):[20b] A round-bottomed flask was charged with (*S*,*S*)-**13**·2 C_7H_8 (0.1058 g, 0.0476 mmol)[20b] and acetone (3 mL) under ambient conditions. Then solid Na(acac-F_6) (0.0657 g, 0.0286 mmol) was added with stirring. After 0.5 h, the solvent was removed. The bright brown residue was suspended in pentane (1–2 mL). The mixture was filtered through a plug of silica (2 cm × 10 cm) with pentane (≈15 mL) and then CH_2Cl_2/pentane (2:1 v/v). The orange fractions were collected, and the solvent was removed by oil-pump vacuum (5×10^{-3} mbar, 1 day) to give (*S*)-**16** (0.075 g, 0.034 mmol, 72%) as a yellow-orange powder, m.p. 124–125 °C (capillary); DSC: endotherm, T_i 95.8 °C, T_e 102.4 °C, T_p 115.8 °C, T_c 123.6 °C, T_f 150.0 °C; exotherm, T_e 214.4 °C; TGA: onset of mass loss, T_i 219.2 °C. Elemental analysis calcd (%) for $C_{41}H_{32}F_6NOP_2PdRe$ (1055.27): C 46.66, H 3.05, N 1.32; found: C 46.62, H 3.22, N 1.32; $[\alpha]_{25}^{589} = -44°\pm3°$ (c = 1.21 mg mL^{-1}, THF); ^{1}H NMR (400 MHz, C_6D_6): δ = 8.19–8.14 (m, 2H of 5 C_6H_5), 7.47–7.42 (m, 8H of 5 C_6H_5), 7.26–7.22 (m, 2H of 5 C_6H_5), 7.11–7.07 (m, 1H of 5 C_6H_5), 7.00–6.91 (m, 12H of 5 C_6H_5), 6.02 (s, 1H, $CH(COCF_3)_2$), C_5H_4 at 5.37 (brs, 1H), 4.98 (m, 1H), 4.79 (m, 1H), 3.18 (brs, 1H); 3.05–2.99 (m, 1H, C*H*H′), 2.55–2.45 ppm (m, 1H, CH*H*′); ^{13}C{^{1}H} NMR (101 MHz, C_6D_6): δ = 175.4 (vbrm, *C*OCF_3), PPh_3 at 136.7 (d, ^1J(C,P) = 51 Hz, *i*), 133.7 (d, ^2J(C,P) = 11 Hz, *o*), 130.1 (d, ^4J-(C,P) = 2 Hz, *p*), 128.6 (d, ^3J(C,P) = 10 Hz, *m*); PPhPh′ at 138.6 (d, ^1J-(C,P) = 30 Hz, *i*), 134.0 (d, ^2J(C,P) = 10 Hz, *o*), 132.3 (d, ^1J(C,P) = 59 Hz, *i*′), 131.6 (d, ^2J(C,P) = 9 Hz, *o*′), 130.9 (d, ^2J(C,P) = 3 Hz, *p*), 123.0 (d, ^2J(C,P) = 3 Hz, *p*′), 128.8 (d, ^3J(C,P) = 11 Hz, *m*);[45] 115.3 (q, ^1J(C,F) = 3 Hz, CF_3),[54] 90.1 (brs, *C*$H(COCF_3)_2$), C_5H_4 at 120.5 (m), 94.0 (m), 90.3 (s), 89.8 (s), 87.1 (s); −15.4 ppm (d, ^1J(C,P) = 20 Hz, CH_2); ^{31}P{^{1}H} NMR (162 MHz, C_6D_6): δ = 62.7 (d, ^3J(P,P) = 21 Hz, PPh_2), 23.6 ppm (d, ^3J(P,P) = 21 Hz, PPh_3); ^{19}F NMR (282 MHz, C_6D_6): δ = −70.8 (s, 3F, CF_3), −71.4 ppm (s, 3F, CF_3′); IR (powder film): $\tilde{\nu}$ = 1633 cm^{-1} (s, NO); MS:[42] 1055 (100) [**16**]$^+$, 848 (10) [(η^5-C_5H_4)Re(NO)-(PPh_3)(CH_2PPh_2)Pd]$^+$, 742 (45) [(η^5-C_5H_4)Re(NO)(PPh_3) (CH_2PPh_2)]$^+$.

(*S*)-[(η^5-C_5H_4)Re(NO)(PPh_3)(μ-CH_2PPh_2)Pd(NC_5H_5)(Br)] ((*S*)-17b): A round-bottomed flask was charged with (*S*,*S*)-**10b** (0.038 g, 0.020 mmol) and benzene (5 mL) under ambient conditions. Then pyridine (0.2 mL) was added with stirring, giving a yellow solution. After 0.5 h, pentane (25 mL) was added. The supernatant was decanted from the yellow powder, which was dissolved in $CHCl_3$ (2 mL). One drop of pyridine was added, and the solution was layered gently with pentane (10 mL). After 2 days, the supernatant was decanted from the yellow needles, which were washed with pentane and dried under a N_2 stream to give (*S*)-**17b**·$CHCl_3$ (0.0329 g, 0.029 mmol, 72%). NMR spectra showed two geometric isomers (*SP*-4-2, *SP*-4-4)[23] and an equilibrium with (*S*,*S*)-**10b** and pyridine (0.3 M in $CDCl_3$: (78±5):(22±5) (*S*)-**17b**/(*S*,*S*)-**10b**). DSC: exotherm, T_i 66.4 °C, T_e 66.9 °C, T_p 67.5 °C, T_c 68.7 °C, T_f 70.6 °C; endotherm, T_i 74.0 °C, T_e 78.5 °C, T_p 106.5 °C, T_c 126.7 °C, T_f 130.2 °C; endotherm, T_i 131.9 °C, T_e 133.6 °C, T_p 140.8 °C, T_c 147.7 °C, T_f 150.2 °C; TGA: onset of first mass loss regime, T_i 38.4 °C, T_f 103.8 °C (3.4% mass loss; theory for 1 $CHCl_3$ 10.6%); onset of second mass loss regime, T_i 175.1 °C, T_f 230.0 °C (5.9% mass loss; theory for 1 $CHCl_3$ 10.6%); onset of third mass loss regime, T_i 251.2 °C. Elemental analysis calcd (%) for $C_{41}H_{36}N_2OP_2BrPdRe$·$CHCl_3$ (1126.6): C 44.77, H 3.31, N 2.48; found: C 44.41, H 3.46, N 2.38; ^{1}H NMR (400 MHz, $CDCl_3$, (*S*)-**17b** signals only): δ = 8.8–6.8 (m, C_6H_5 and NC_5H_5), C_5H_4 at 5.48 (brs, 1H),[55] 5.33/5.24 (2 × brs, 67:33, 1H), 5.08/4.87 (2 × brs, 67:33, 1H), 3.12/2.71 (2 × brs, 67:33, 1H); 3.02–2.86 (m, 1H, C*H*H′),[55] 2.27–2.09 ppm (m, 1H, CH*H*′);[55] ^{31}P{^{1}H} NMR (162 MHz, $CDCl_3$, (*S*)-**17b** signals only): δ = 67.9 (d, ^3J(P,P) = 24 Hz, PPh_2, major isomer, ≈67%), 67.1 (d, ^3J(P,P) = 22 Hz, PPh_2, minor isomer, ≈33%), 24.1 (d, ^3J(P,P) = 25 Hz, PPh_3, major isomer, ≈67%), 23.3 ppm (d, ^3J(P,P) = 22 Hz, PPh_3, minor isomer, coincident with a signal of (*S*,*S*)-**10b**); IR (powder film): $\tilde{\nu}$ = 1741 cm^{-1} (s, NO); MS:[42] 928 (5) [(η^5-C_5H_4)Re(NO)(PPh_3)-(CH_2PPh_2)Pd(Br)]$^+$, 848 (10) [(η^5-C_5H_4)Re(NO)(PPh_3)(CH_2PPh_2)Pd]$^+$, 742 (10) [(η^5-C_5H_4)Re(NO)(PPh_3)(CH_2PPh_2)]$^+$.

Suzuki–Miyaura reactions (Table 3): The following procedure was representative. A Schlenk tube was charged sequentially with $PhB(OH)_2$ (1.830 g, 15.00 mmol), K_3PO_4 (4.25 g, 20.00 mmol), toluene (20 mL), 4-bromoacetophenone (1.99 g, 10.00 mmol), tridecane (1.22 mL, 5.00 mmol), and a solution of **10b** in toluene (0.000050 M; 1.0 mL, 5.0×10^{-5} mmol) with vigorous stirring. Then it was fitted with a condenser and placed in an 80 °C oil bath. Aliquots (≈0.2 mL) were assayed periodically by GC. The identity of the product was confirmed by comparison of the GC retention time on two different columns with that of an authentic sample.

Mizoroki–Heck reactions (see Supporting Information): The following procedure was representative. A Schlenk tube was charged sequentially with 4-bromoacetophenone (0.1991 g, 1.00 mmol), NaOAc (0.1148 g, 1.40 mmol), (nBu)$_4$N$^+$ Br$^-$ (0.0645 g, 0.200 mmol), di(2-*n*-butoxyethyl) ether (0.1111 g, 0.509 mmol), DMF (6 mL), methyl acrylate (0.20 mL, 2.22 mmol), and a solution of (*S*,*S*)-**10b** in DMF (0.000119 M; 0.050 mL, 5.93×10^{-6} mmol), fitted with a septum, and placed in a 140 °C oil bath. The orange-brown suspension was stirred vigorously and monitored by GC. The identity of the product was confirmed by comparison of the GC retention time on two different columns with that of an authentic sample.

Transmission electron microscopy: An aliquot (0.1 mL) was taken from the Mizoroki–Heck reaction of methyl acrylate and 4-iodotoluene using (*S*)-**16** (entry 4, Scheme 8 in Supporting Information) and poured into diethyl ether (1 mL). A drop was transferred to the surface of a carbon covered copper TEM grid, which was dried under vacuum at 70 °C. Images were recorded on a Philips CM 300 UT microscope.

Crystallography

Complex **11b** was dissolved in CH_2Cl_2 and layered with ether. After three days, yellow prisms of **11b**·2 CH_2Cl_2 were analyzed as outlined in Table 1.[56] Cell parameters were obtained from 15 reflections using a 10° scan and refined with 25 reflections. Lorentz, polarization, and absorption corrections were applied.[57] The space group was determined from systematic absences and subsequent least-squares refinement. The structure was solved by direct methods. The parameters were refined with all the data by full-matrix least-squares on F^2 using SHELXL-97.[58] Non-hydrogen atoms were refined with anisotropic thermal parameters. The hydrogen atoms were fixed in idealized positions using a riding model. Scattering factors were taken from the literature.[59]

Complex (*S*)-**6c**[20c] was dissolved in benzene and layered with hexanes. After three days, the red cubes were analyzed as described for **11b**·2 CH_2Cl_2 (cell parameters from 10 frames using a 10° scan; refined with 2960 reflections). The structure was solved and refined as described for **11b**·2 CH_2Cl_2. The absolute configuration was confirmed by Flack's parameter (Table 1; theory for correct and inverted structures, 0 and 1).[60]

Crystals of (*S*,*S*)-**13**·2 C_7H_8 (see above) and (*R*,*R*)-**13**·2 C_7H_8 were analyzed as described for **11b**·2 CH_2Cl_2 (cell parameters from 10 frames using a 10° scan; refined with 10766–10823 reflections). The structures were solved and refined as described for **11b**·2 CH_2Cl_2.

Some $CHCl_3$ was added to a concentrated CH_2Cl_2 solution of (*S*,*S*)-**10b**. The mixture was layered gently with pentane. After one day, yellow needles of (*S*,*S*)-**10b**·CH_2Cl_2·2$CHCl_3$ were analyzed as described for **11b**·2CH_2Cl_2 (cell parameters from 10 frames using a 10° scan; refined with 5101 reflections). The structure was solved and refined as described for **11b**·2CH_2Cl_2. The CH_2Cl_2 molecules showed site disorder (50:50) about an inversion center.

Crystals of (*S*)-**17b**·$CHCl_3$ (see above) were analyzed as described for **11b**·2CH_2Cl_2 (cell parameters from 10 frames using a 10° scan; refined with 5334 reflections). The structure was solved and refined as described for **11b**·2CH_2Cl_2.

CCDC-290483 (**11b**·2CH_2Cl_2), CCDC-290482 ((*S*)-**6c**), CCDC-290479 ((*S*,*S*)-**13**·2C_7H_8), CCDC-270134 ((*R*,*R*)-**13**·2C_7H_8), CCDC-290481 ((*S*,*S*)-**10b**·CH_2Cl_2·2$CHCl_3$), and CCDC-290480 ((*S*)-**17b**·$CHCl_3$) contain the supplementary crystallographic data for this paper. These data can be obtained free of charge from the Cambridge Crystallographic Data Centre via www.ccdc.cam.ac.uk/data_request/cif. For ease of comparison (for example, in Table 2), the atom numbers in some of the structures described in the present work have been changed from those in the CCDC archives.

Acknowledgements

We thank the Deutsche Forschungsgemeinschaft (DFG, 300/4-2) and Johnson Matthey PMC (palladium loans) for support, and Dr. O. Delacroix for valuable experimental assistance.

[1] a) A. C. Cope, R. W. Siekman, *J. Am. Chem. Soc.* **1965**, *87*, 3272; b) A. C. Cope, E. C. Friedrich, *J. Am. Chem. Soc.* **1968**, *90*, 909.
[2] Reviews: a) R. B. Bedford, *Chem. Commun.* **2003**, 1787; b) I. P. Beletskaya, A. V. Cheprakov, *J. Organomet. Chem.* **2004**, *689*, 4055; c) J. Dupont, C. S. Consorti, J. Spencer, *Chem. Rev.* **2005**, *105*, 2527.
[3] V. Farina, *Adv. Synth. Catal.* **2004**, *346*, 1553.
[4] a) T. K. Hollis, L. E. Overman, *Tetrahedron Lett.* **1997**, *38*, 883; b) F. Cohen, L. E. Overman, *Tetrahedron: Asymmetry* **1998**, *9*, 3213; c) Y. Donde, L. E. Overman, *J. Am. Chem. Soc.* **1999**, *121*, 2933; d) J. Kang, K. H. Yew, T. H. Kim, D. H. Choi, *Tetrahedron Lett.* **2002**, *43*, 9509; e) C. E. Anderson, Y. Donde, C. J. Douglas, L. E. Overman, *J. Org. Chem.* **2005**, *70*, 648; f) A. Moyano, M. Rosol, R. M. Moreno, C. López, M. A. Maestro, *Angew. Chem.* **2005**, *117*, 1899; *Angew. Chem. Int. Ed.* **2005**, *44*, 1865.
[5] a) L. E. Overman, C. E. Owen, M. M. Pavan, C. J. Richards, *Org. Lett.* **2003**, *5*, 1809; b) J. Kang, T. H. Kim, K. H. Yew, W. K. Lee, *Tetrahedron: Asymmetry* **2003**, *14*, 415; c) C. E. Anderson, L. E. Overman, *J. Am. Chem. Soc.* **2003**, *125*, 12412; d) S. F. Kirsch, L. E. Overman, M. P. Watson, *J. Org. Chem.* **2004**, *69*, 8101; e) S. F. Kirsch, L. E. Overman, *J. Am. Chem. Soc.* **2005**, *127*, 2866; f) R. S. Prasad, C. E. Anderson, C. J. Richards, L. E. Overman, *Organometallics* **2005**, *24*, 77; g) S. F. Kirsch, L. E. Overman, *J. Org. Chem.* **2005**, *70*, 2859.
[6] a) P. Barbaro, C. Bianchini, G. Giambastiani, S. L. Parisel, *Coord. Chem. Rev.* **2004**, *248*, 2131, and earlier reviews of ferrocenyl-containing catalysts cited therein; b) survey of non-metallocene architectural units: O. Delacroix, J. A. Gladysz, *Chem. Commun.* **2003**, 665.
[7] a) K. Kromm, B. D. Zwick, O. Meyer, F. Hampel, J. A. Gladysz, *Chem. Eur. J.* **2001**, *7*, 2015; b) K. Kromm, F. Hampel, J. A. Gladysz, *Organometallics* **2002**, *21*, 4264; c) K. Kromm, P. L. Osburn, J. A. Gladysz, *Organometallics* **2002**, *21*, 4275.
[8] a) L. J. Alvey, O. Delacroix, C. Wallner, O. Meyer, F. Hampel, S. Szafert, T. Lis, J. A. Gladysz, *Organometallics* **2001**, *20*, 3087; b) K. Kromm, F. Hampel, J. A. Gladysz, *Helv. Chim. Acta* **2002**, *85*, 1778; c) K. Kromm, S. Eichenseher, M. Prommesberger, F. Hampel, J. A. Gladysz, *Eur. J. Inorg. Chem.* **2005**, *15*, 2983.
[9] a) S. Eichenseher, O. Delacroix, K. Kromm, F. Hampel, J. A. Gladysz, *Organometallics* **2005**, *24*, 245; b) J. Giner Planas, F. Hampel, J. A. Gladysz, *Chem. Eur. J.* **2005**, *11*, 1402.
[10] F. K. Friedlein, F. Hampel, J. A. Gladysz, *Organometallics* **2005**, *24*, 4103.
[11] a) V. I. Sokolov, L. L. Troitskaya, O. A. Reutov, *J. Organomet. Chem.* **1977**, *133*, C28; b) C. López, R. Bosque, X. Solans, M. Font-Bardia, *Tetrahedron: Asymmetry* **1996**, *7*, 2527; c) I. A. Mamedyarova, M. N. Nefedova, V. I. Sokolov, *J. Organomet. Chem.* **1996**, *524*, 181; d) V. V. Dunina, O. N. Gorunova, M. V. Livantsov, Y. K. Grishin, L. G. Kuz′mina, N. A. Kataeva, A. V. Churakov, *Inorg. Chem. Commun.* **2000**, *3*, 354; V. V. Dunina, O. N. Gorunova, M. V. Livantsov, Y. K. Grishin, L. G. Kuz′mina, N. A. Kataeva, A. V. Churakov, *Tetrahedron: Asymmetry* **2000**, *11*, 3967; e) F. X. Roca, M. Motevalli, C. J. Richards, *J. Am. Chem. Soc.* **2005**, *127*, 2388; f) L. L. Troitskaya, Z. A. Starikova, T. V. Demeshchik, S. T. Ovseenko, E. V. Vorontsov, V. I. Sokolov, *J. Organomet. Chem.* **2005**, *690*, 3976.
[12] a) A. M. Stevens, C. J. Richards, *Organometallics* **1999**, *18*, 1346; b) G. Jones, C. J. Richards, *Organometallics* **2001**, *20*, 1251.
[13] A. Berger, J.-P. Djukic, M. Pfeffer, J. Lacour, L. Vial, A. de Cian, N. Kyritsakas-Gruber, *Organometallics* **2003**, *22*, 5243, and earlier work cited therein.
[14] a) A. D. Ryabov, *Chem. Rev.* **1990**, *90*, 403; b) W. A. Herrmann, C. Brossmer, C.-P. Reisinger, T. H. Riermeier, K. Öfele, M. Beller, *Chem. Eur. J.* **1997**, *3*, 1357; c) D. L. Davies, S. M. A. Donald, S. A. Macgregor, *J. Am. Chem. Soc.* **2005**, *127*, 13754.
[15] Compound numbers that are indexed **a**, **b**, and **c** indicate chloride, bromide, and iodide derivatives, respectively.
[16] a) W. A. Herrmann, *Chem. Ber.* **1978**, *111*, 2458; b) L. V. Dinh, F. Hampel, J. A. Gladysz, *J. Organomet. Chem.* **2005**, *690*, 493.
[17] a) J. J. Kowalczyk, A. M. Arif, J. A. Gladysz, *Chem. Ber.* **1991**, *124*, 729; b) P. C. Heah, A. T. Patton, J. A. Gladysz, *J. Am. Chem. Soc.* **1986**, *108*, 1185 (see Scheme 2).
[18] M. A. Dewey, Y. Zhou, Y. Liu, J. A. Gladysz, *Organometallics* **1993**, *12*, 3924.
[19] K. Kromm, Doctoral Dissertation, Universität Erlangen–Nürnberg, **2003**.
[20] a) When both enantiomers were prepared, the synthesis of only one is given in the Experimental Section. b) Only (*S*,*S*)-**10a**, (*R*,*R*)-**10c**, and (*R*)-**16** were prepared. The configurations of the last two are the opposite of those normally depicted in papers in this series. To facilitate comparisons, their configurations (and those of the necessary educts) have been inverted throughout this paper. c) The crystal structure of (*R*)-**6c** was determined, and not (*S*)-**6c** as represented throughout this paper.
[21] a) C. W. K. Gstöttmayr, V. P. W. Böhm, E. Herdtweck, M. Grosche, W. A. Herrmann, *Angew. Chem.* **2002**, *114*, 1421; *Angew. Chem. Int. Ed.* **2002**, *41*, 1363; b) C. Dai, G. C. Fu, *J. Am. Chem. Soc.* **2001**, *123*, 2719.
[22] The only exception is (*S*,*S*)-**13** below (δ = 4.78–5.54). Here, the crystal structure shows a distance of 4.145 Å between the centroid of the PPh_3 phenyl ring *syn* to the cyclopentadienyl ligand and the closest cyclopentadienyl carbon (α to the Pd–C bond). In contrast, the three other crystallographically characterized palladacycles show distances of 3.735–3.878 Å.
[23] The terms *SP*-4-2, *SP*-4-3, and *SP*-4-4 are used to distinguish the three stereoisomers of square planar complexes of formula MLL′L″L‴ (*SP*-4 = square planar; -2, -3, and -4 indicate that the groups with the second, third, or fourth highest Cahn–Ingold–Prelog priorities are *trans* to the group with the highest priority): *Nomenclature of Inorganic Chemistry: IUPAC Recommendations 2005* (Eds.: N. G. Connely, T. Damhus, R. M. Hartshorn, A. T. Hutton), Royal Society of Chemistry, London, **2005**, pp. 179–181.
[24] a) L. Yu. Ukhin, N. A. Dolgopolova, L. G. Kuz′mina, Yu. T. Struchkov, *J. Organomet. Chem.* **1981**, *210*, 263; b) R. Giri, J. Liang, J.-G. Lei, J.-J. Li, D.-H. Wang, X. Chen, I. C. Naggar, C. Guo, B. M. Foxman, J.-Q. Yu, *Angew. Chem.* **2005**, *117*, 7586; *Angew. Chem. Int. Ed.* **2005**, *44*, 7420.

[25] a) Y. Fuchita, K. Hiraki, Y. Matsumoto, *J. Organomet. Chem.* **1985**, *280*, C51; b) M. Pfeffer, E. Wehman, G. van Koten, *J. Organomet. Chem.* **1985**, *282*, 127; c) G. Balavoine, J. C. Clinet, *J. Organomet. Chem.* **1990**, *390*, C84; d) M. T. Alonso, O. Juanes, J. de Mendoza, J. C. Rodríguez-Ubis, *J. Organomet. Chem.* **1992**, *430*, 349.
[26] T. Murahashi, H. Kurosawa, *Coord. Chem. Rev.* **2002**, *231*, 207.
[27] Note that with respect to the Pd–Pd–Pd axis, the PPh_2 unit on one terminus is *anti* to the cyclopentadienyl unit on the other.
[28] F. B. Ogilvie, J. M. Jenkins, J. G. Verkade, *J. Am. Chem. Soc.* **1970**, *92*, 1970.
[29] W. H. Hersh, *J. Chem. Educ.* **1997**, *74*, 1485.
[30] J. P. Wolfe, R. A. Singer, B. H. Yang, S. L. Buchwald, *J. Am. Chem. Soc.* **1999**, *121*, 9550.
[31] a) M. T. Reetz, E. Westermann, *Angew. Chem.* **2000**, *112*, 170; *Angew. Chem. Int. Ed.* **2000**, *39*, 165; b) C. Rocaboy, J. A. Gladysz, *New J. Chem.* **2003**, *27*, 39, and references therein; c) C. C. Cassol, A. P. Umpierre, G. Machado, S. I. Wolke, J. Dupont, *J. Am. Chem. Soc.* **2005**, *127*, 3298, and references therein; d) D. Astruc, F. Lu, J. R. Aranzaes, *Angew. Chem.* **2005**, *117*, 8062; *Angew. Chem. Int. Ed.* **2005**, *44*, 7852.
[32] For additional palladacycles that have been shown by other types of experimental data to give nonmolecular catalysts, see: a) J. G. de Vries, *Dalton Trans* **2006**, 421; b) M. R. Eberhard, *Org. Lett.* **2004**, *6*, 2125; c) K. Yu, W. Sommer, J. M. Richardson, M. Weck, C. W. Jones, *Adv. Synth. Catal.* **2005**, *347*, 161; d) D. E. Bergbreiter, P. L. Osburn, J. D. Frels, *Adv. Synth. Catal.* **2005**, *347*, 172; e) M. Rosol, A. Moyano, *J. Organomet. Chem.* **2005**, *690*, 2291.
[33] R. Imbos, A. J. Minnaard, B. L. Feringa, *J. Am. Chem. Soc.* **2002**, *124*, 184.
[34] F. K. Friedlein, Doctoral Dissertation, Universität Erlangen–Nürnberg, **2006**.
[35] a) R. B. Bedford, S. L. Hazelwood, P. N. Horton, M. B. Hursthouse, *Dalton Trans.* **2003**, 4164; b) F. d'Orlyé, A. Jutand, *Tetrahedron* **2005**, *61*, 9670.
[36] A. D. Ryabov, G. M. Kazankov, S. A. Kurzeev, P. V. Samuleev, V. A. Polyakov, *Inorg. Chim. Acta* **1998**, *280*, 57.
[37] Representative recent papers: a) S. U. Son, Y. Jang, J. Park, H. B. Na, H. M. Park, H. J. Yun, J. Lee, T. Hyeon, *J. Am. Chem. Soc.* **2004**, *126*, 5026; b) C. Bock, C. Paquet, M. Couillard, G. A. Botton, B. R. MacDougall, *J. Am. Chem. Soc.* **2004**, *126*, 8028; c) M. Chen, J. P. Liu, S. Sun, *J. Am. Chem. Soc.* **2004**, *126*, 8394; d) J. Park, M. G. Kim, Y. Jun, J. S. Lee, W. Lee, J. Cheon, *J. Am. Chem. Soc.* **2004**, *126*, 9072; e) K. H. Park, Y. K. Chung, *Adv. Synth. Catal.* **2005**, *347*, 854.
[38] M. A. Dewey, J. A. Gladysz, *Organometallics* **1993**, *12*, 2390.
[39] H. K. Cammenga, M. Epple, *Angew. Chem.* **1995**, *107*, 1284; *Angew. Chem. Int. Ed. Engl.* **1995**, *34*, 1171.
[40] A. F. Burchat, J. M. Chong, N. Nielsen, *J. Organomet. Chem.* **1997**, *542*, 281.
[41] The quality of commercial $Ph_3C^+X^-$ can vary, and crystallization from CH_2Cl_2/hexanes or CH_2Cl_2/benzene is recommended: A. T. Patton, C. E. Strouse, C. B. Knobler, J. A. Gladysz, *J. Am. Chem. Soc.* **1983**, *105*, 5804.
[42] FAB, 3-NBA, *m/z* (%); the peaks correspond to the most intense signal of the isotope envelope.
[43] F. Agbossou, E. J. O'Connor, C. M. Garner, N. Quirós Méndez, J. M. Fernández, A. T. Patton, J. A. Ramsden, J. A. Gladysz, *Inorg. Synth.* **1992**, *29*, 211.
[44] The reaction mixture was checked by TLC at this stage. If the educt (*S*)-**8** remained, column chromatography (SiO_2, toluene/hexanes (1:1 v/v)) was performed.
[45] Some or all of the PPh_3 or PPhPh′ *meta*-carbon signals were obscured by C_6D_6.
[46] Measured gravimetrically inside a glove box (difference in mass between loaded and discharged syringe).
[47] The four downfield lines of this ddd were obscured by the PPh_3 and PPh_2 signals.
[48] The minor signals were absent in the ^{1}H NMR spectra of (*S*,*S*)-**10b** and were assigned to the *meso* diastereomer.
[49] These (broadened) resonances were tentatively assigned to both *syn* and *anti* isomers (overlapping signals). However, in some cases nonoverlapping signals of the minor isomer may have been be too broad or too weak to observe.
[50] Some or all of the PPhPh′ or C_5H_4 ^{13}C NMR signals were too weak to observe.
[51] It was not possible to assign signals to the $RePPh_3$ vs $PdPPh_3$ phenyl groups; the designations *i*/*o*/*m*/*p* and *i*′/*o*′/*m*′/*p*′ are arbitrary.
[52] This surprisingly large coupling constant has been verified in another solvent ($CDCl_3$) and by a 500 MHz spectrum. It may result from a "W" conformational relationship between the CH_2PPh_2 phosphorus atom and the methyl group of the *cis* acetate ligand.
[53] S. Eichenseher, Doctoral Dissertation, Universität Erlangen–Nürnberg, **2005**. The synthesis is analogous to that of the racemate.[9a]
[54] Only one CF_3 ^{13}C NMR signal was detected.
[55] This signal overlaps with one of (*S*,*S*)-**10b**. Therefore, the intensity reflects the theoretical rather than a measured value.
[56] When the crystals were dried by either vacuum or a nitrogen stream, the solvent of crystallization was removed.
[57] a) "Express" Enraf-Nonius diffractometer control software, Release 5.1, Enraf-Nonius, Delft, The Netherlands, **1994** (**11b**·2 CH_2Cl_2), or "Collect" data collection software, B. V. Nonius, **1998** (other structures); b) "Scalepack" data processing software: Z. Otwinowski, W. Minor, *Methods in Enzymology* **1997**, *276* (Macromolecular Crystallography, Part A), 307.
[58] G. M. Sheldrick, SHELX-97, Program for refinement of crystal structures, University of Göttingen, **1997**.
[59] D. T. Cromer, J. T. Waber, in *International Tables for X-ray Crystallography* (Eds.: J. A. Ibers, W. C. Hamilton), Kynoch, Birmingham, UK, **1974**.
[60] H. D. Flack, *Acta Crystallogr. Sect. A* **1983**, *39*, 876.

Received: December 9, 2005
Published online: April 21, 2006

